liver (3), abdominal wall (1) and lung (1). Of the 33 FNA cases, 30 were primary AML (28 in kidney and 2 in liver) and 3 were metastasis (in liver, lung and abdominal wall, respectively). FNA diagnoses included consistent with or favor AML (16, 49%), descriptive (13), non-diagnostic (1) and erroneous diagnosis (3). Of the latter 3 cases (all in the kidney), two were called "clear cell renal cell carcinoma" due to predominant epithelioid component and one was called "pleomorphic malignancy". Two renal AMLs had co-existing metastatic carcinoma (neuroendocrine carcinoma from pancreas and metastatic lung adenocarcinoma, respectively).
Upon review, smooth muscle component was most commonly seen (19), followed by vascular component (17) and adipose tissue (6). Only 4 cases showed all the three components; 13 cases had 2 components and 7 cases had smooth muscle component only. Fifteen cases showed epithelioid smooth muscle component, 7 of which were predominantly epithelioid including all extra-renal cases (4) and erroneous cases (3). Eight of the 13 cases with descriptive diagnosis have epithelioid component. Of the 33 FNA cases, 19 had contributory cell block and 9 had smear only. Immunostains were performed in 11 cases (10 on cell block and one on smear) and led to AML diagnosis in 9 cases. Positive expression of HMB45 was found in 8 of 10, Melan-A in 4 of 4 and SMA in 4 of 4 cases. No immunostaining was performed on the 3 erroneous cases.
Conclusions: FNA diagnosis of AML may be challenging, especially when it has extra-renal location (as primary or metastatic) and/or shows epithelioid component. Immunostaining is important to improve diagnostic accuracy of this rare entity.

486 Next Generation Sequencing of NSCLC in EBUS-FNA vs. Corresponding FFPE Samples

Yaolin Zhou, Jordan P Reynolds, Maureen A Jakubowski, Zhen Wang, Patrick C Feasel, Roger D Klein, Yu-Wei Cheng. Cleveland Clinic, Cleveland, OH.
Background: Next Generation Sequencing (NGS) on endoscopic ultrasound-guided fine needle aspiration (EBUS-FNA) samples is useful for facilitating treatment decisions of non-small cell lung cancer (NSCLC) patients. We assessed the effectiveness of detecting driver mutations by NGS in surgical and biopsy tissue versus liquid based cytology (LBC) specimens.
Design: Archived extracted DNA from residual cell pellets of LBC specimens (method previously described) with known *EGFR* and *KRAS* mutation status were retrieved. For each case, DNA from corresponding formalin-fixed paraffin-embedded (FFPE) tissue was also extracted. Mutation hotspot NGS libraries for *BRAF, EGFR, ERBB2, FGFR1, KRAS, MET*, and *PIK3C* were prepared on all DNA samples, sequenced by Illumina MiSeq and analyzed using NextGENe software with reference genome hg19. Each patient's NGS variant calls were compared between FFPE and LBC results. *EGFR* and *KRAS* results were also compared against prior real-time PCR results (Qiagen).
Results: Ten patients from June to August 2014 had adequate DNA in both LBC and FFPE specimens as measured by Qubit™ fluorometric quantitation. LBC samples were obtained from EBUS-FNA (9) or bronchial washing (1). Ten corresponding FFPE tissue specimens (6 transbronchial biopsies, 2 lobectomies, 1 each of brain and bone metastases) were selected for sequencing.

Pathologic Diagnosis	Mutation Status	Cytology Specimen	FFPE Tissue Specimen
Poorly differentiated adenocarcinoma	*KRAS*-	EBUS-FNA	Transbronchial Biopsy
Adenocarcinoma with solid (70%) and acinar (30%) patterns	c.34G>T p.Gly12Cys	EBUS-FNA	Transbronchial Biopsy
Adenocarcinoma, solid predominant	*KRAS*-	EBUS-FNA	Lobectomy
Adenocarcinoma	*KRAS*-	EBUS-FNA	Transbronchial Biopsy
Adenocarcinoma	c.35G>A, p.Gly12Asp	Bronchial Washing	Transbronchial Biopsy
Adenocarcinoma	c.34G>A, p.Gly12Ser	EBUS-FNA	Transbronchial Biopsy
Poorly differentiated NSCLC favor adenocarcinoma	*KRAS* - *ALK* t(2p23) by FISH	EBUS-FNA	Transbronchial Biopsy
Poorly differentiated w/ squamous differentiation	*KRAS*-	EBUS-FNA	Tibial Reamings
Adenocarcinoma, solid predominant	c.34G>T, p.Gly12Cys	EBUS-FNA	Lobectomy
Poorly differentiated adenocarcinoma	*KRAS*-	EBUS-FNA	Brain Excision

The average DNA concentration for LBC samples was 43.2 ng/µl and FFPE was 12.3 ng/µl. Mean average read depths were 10,899 and 7,980 for LBC and FFPE, respectively. Five FFPE and 1 LBC specimens had minimum read depths below quality control standards (<100) involving primarily *PIK3CA* (6) and *BRAF* (3).
Targeted genes were concordant across specimen types. For both FFPE and LBC, NGS detected *KRAS* mutations previously identified by PCR. In addition, all 20 specimens showed a common *EGFR* polymorphism c.2361G>A.
Conclusions: NGS results of FFPE and LBC (DNA from cell pellets) were consistent, but the superior coverage depth of LBC specimens supports its clinical use. Our initial experience using NGS on 128 clinical lung cancer FNAs detected *KRAS* mutations in 30 patients and *EGFR* in 16; qualifying 8 for tyrosine kinase inhibitor therapy. Thus, the clinical utility of NGS on EBUS-FNA derived LBC samples appears promising.

Dermatopathology

487 Validation of a New SNP-Array Platform as an Ancillary Tool for the Diagnosis of Difficult Melanocytic Lesions

Ahmed Alomari, Paul W Harms, Lori Lowe, Douglas R Fullen, Rajiv Patel, Alexandra Hristov, May P Chan, Min Wang, Aleodor A Andea. University of Michigan Health System, Ann Arbor, MI.
Background: Atypical melanocytic tumors that defy classification as benign or malignant using pathological criteria alone are not uncommon. Additional ancillary tests are often needed to enhance diagnostic accuracy. Prior studies have shown that evaluation of copy number variations (CNV) by array comparative genomic hybridization can be used to assist in differentiating nevi from melanomas. The performance of this technique in ambiguous melanocytic lesions and its correlation with clinical outcomes are yet to be fully characterized. More recently, platforms based on single nucleotide polymorphism arrays (SNP) arrays have become available; however, experience with their use in melanocytic lesions is limited. Herein we aim to evaluate the performance of a SNP-array on a cohort of benign, malignant and ambiguous melanocytic tumors with clinical follow-up.
Design: Eighty five melanocytic lesions were included. Using histopathological examination and immunohistochemistry, the cases were classified into four categories; benign nevi, atypical nevi, ambiguous lesions and melanomas. Follow-up data was gathered from our institutional electronic health record system and adverse events including sentinel lymph node metastasis, local recurrence, distant metastasis or death were recorded. Tissue from unstained slides or tissue rolls was processed and analyzed for CNV and loss of heterozygosity using the OncoScan V3 SNP-array platform (Affymetrix).
Results: Follow-up data was available in 57 patients (mean 5.9 months). 6/6 benign nevi (100%) and 12/15 (80%) atypical nevi showed no significant CNVs. None of these patients with follow up data had adverse events. 14/24 (58%) ambiguous lesions and 36/40 (90%) melanomas showed at least one significant alteration. In the ambiguous group, lymph node metastases were detected in 2/3 (66%) of patients with CNVs and 0/2 (0%) of patients without CNVs. The average number of CNVs in melanoma patients with or without adverse outcome was 23.4 versus 12.7, respectively. The average number of CNVs in primary versus metastatic lesions was 17.7 versus 24.5 respectively.
Conclusions: SNP-arrays may improve our diagnostic accuracy in the study of difficult melanocytic lesions. On a limited sample, it may show negative predictive value for lymph node metastasis in ambiguous lesions. In addition, in definitive melanomas, the total number of alterations correlates with adverse outcome.

488 Intratumoral Lymphovascular Invasion Detected by D2-40 Correlates with Metastasis in Primary Cutaneous Merkel Cell Carcinoma

Rami N Al-Rohil, Laurence Feldmeyer, Priyadharsini Nagarajan, Genevieve R Lyons, Jonathan L Curry, Carlos A Torres-Cabala, Doina Ivan, Victor G Prieto, Michael T Tetzlaff, Phyu P Aung. UT MD Anderson Cancer Center, Houston, TX.
Background: Primary Cutaneous Merkel cell carcinoma (MCC) is an aggressive neuroendocrine cancer with a high frequency of metastasis and death. Lymphovascular invasion (LVI) has been shown to correlate with more aggressive phenotype in many tumor types. Here, we examined the significance of LVI detected by D2-40 immunohistochemical (IHC) stain in the prognostic assessment of PCMCC.
Design: We performed a retrospective analysis of 58 patients with PCMCC (1/09-7/14). LVI was determined by H&E and D2-40 IHC. When present, the location (peritumoral or intratumoral) and the size of the vessel were scored. These were compared to LVI by H&E and association with demographic, histologic, Merkel cell polyomavirus status (MCPv) and clinical outcome parameters.
Results: Fifty-eight PCMCC were assessed for LVI using H&E and D2-40. D2-40 increased the detection rate of LVI compared to H&E alone: 44 detected by D2-40 IHC vs. 30 by H&E. D2-40 IHC detected 14 cases missed by H&E, and identified 7 false positive cases by H&E. Histologically the infiltrative growth pattern and non-brisk lymphoid infiltrate were associated with LVI (p=0.005 and 0.055, respectively). In our series, D2-40 detected LVI alone was not associated with metastasis, but intratumoral D2-40 detected LVI was associated with ~4X higher odds of metastasis to any site (p=0.035) and 3.5X greater odds of metastasis beyond the sentinel lymph node (p=0.037) compared to patients without intratumoral LVI.
In addition, tumors with invasion of vessels with a diameter >0.1mm and lesions with intratumoral LVI are each more likely to have invasion beyond skin (p= 0.016 and 0.003, respectively). Patients with MCPv+ MCC tend not to have central LVI (p=0.057).
Conclusions: D2-40 IHC increases the detection of LVI in PCMCC, and intratumoral D2-40 LVI is associated with adverse clinicopathologic parameters of outcome, in

particular, invasion beyond the skin and metastasis. Therefore, we propose D2-40 IHC as a routine method for evaluation of LVI in all PCMCC cases as a predictive marker for metastasis.

489 Laser Microdissection and Mass Spectrometric-Based Proteomic Analysis of Sclerotic Bodies ("Elastocollagenous Balls") in Nephrogenic Systemic Fibrosis

Naziheh Assarzadegan, Michael J Imber, Patrick Vanderboom, Cristine Charlesworth, Wonwoo Shon. University of Florida, Gainesville, FL; Mayo Clinic, Rochester, MN.

Background: Nephrogenic systemic fibrosis occurs in patients with chronic renal disease and it has been linked to previous gadolinium exposure. Microscopically, distinct sclerotic bodies ("elastocollagenous balls") have also been documented in this clinical setting. To date, only few histopathologic data are available for these peculiar cutaneous deposits. The aim of this study is to determine the specific constituents of cutaneous elastocollagenous deposits in nephrogenic systemic fibrosis using laser microdissection and mass spectrometry based proteomic analysis.

Design: Two skin biopsies with characteristic histologic features of nephrogenic systemic fibrosis containing sclerotic bodies were retrieved. In each case, sclerotic bodies were identified and laser microdissected (LMD) using the Leica dissector. These LMD fragments were digested into tryptic peptide and analyzed by nano-flow liquid chromatography electrospray tandem massspectrometry (LC-MS/MS). The informatics analysis was performed using Scaffold (Proteome Software, Portland, OR), where the protein and peptide probability scores were set at 95% and the estimated protein false discovery rate (FDR) was >0.05%.

Results: Microscopically, all skin biopsies showed features of nephrogenic systemic fibrosis characterized by pandermal spindle cell proliferation with increased collagen and scattered sclerotic bodies. Irregularly shaped sclerotic bodies, many of which contained elastic fibers, were present in the dermis and superficial subcutis. Proteomic analysis by LMD-LC-MS/MS was able to accurately identify specific constituents of collagen deposits and entrapped elastic fibers. Both cases showed various collagen types, fibrillin, and microfibril-associated glycoprotein; notably, preferential accumulation of type VI collagen (alpha-1 and alpha-3) and fibrillin was noted. One case also revealed elastin.

Conclusions: In addition to confirming the presence of collagen and elastic fibers, our pilot LMD-LC-MS/MS -based proteomic analysis demonstrated the specific protein contents in sclerotic bodies of nephrogenic systemic fibrosis. A larger number of cases of sclerotic bodies with additional features, such as osseous metaplasia or calcification, will be necessary to more fully understand their exact nature and significance.

490 Prognostic Significance of Regression in Patients with Thin Primary Cutaneous Melanoma

Phyu P Aung, Sanjita Ravishankar, Kenneth Friedman, Denai R Milton, Jonathan L Curry, Carlos A Torres-Cabala, Doina Ivan, Michael T Tetzlaff, Jeffery E Gershenwald, Victor G Prieto, Priyadharsini Nagarajan. UT MD Anderson Cancer Center, Houston, TX.

Background: Regression in melanoma is defined as the replacement of tumor cells by lymphocytic inflammation, along with attenuation of the epidermis and non-lamellated dermal fibrosis with inflammatory cells, melanophages, and telangiectasia. Whether regression is an adverse prognostic factor in predicting survival in thin (≤1mm) primary cutaneous melanoma (PCM) remains controversial in part because the definition and quantification of regression were not consistent in studies assessing its significance. Here, we examined the correlation between regression and conventional prognostic indicators of outcome in a large series of thin PCM using uniform histologic criteria.

Design: We performed a retrospective analysis of 77 patients with thin PCM in the original biopsy (1/09-12/10). We assessed the extent of regression (focal <50% vs. extensive >50%) as well as thickness and correlated these with histologic, demographic and clinical outcome parameters. We measured maximum thickness of regression with a calibrated ocular micrometer from the granular layer of the epidermis (if the lesion was ulcerated from the base of the ulcer) to the deepest point of (1) dermal fibrosis and (2) lymphocytic infiltrate.

Results: The extent of regression (focal vs. extensive) was significantly associated with high Clark level (p=0.01), increased Breslow thickness (p=0.001), increased number of mitotic figures (p=0.05), and presence of vertical growth phase (p=0.04). The depth of regression measured by inflammatory infiltrate significantly associated with high Clark level (p=0.01), increased Breslow thickness (p=0.002), presence of ulceration (p=0.02), and presence of lymphovascular invasion (p=0.04). Significantly reduced overall survival was found in the patients with thin PCM with depth of regression (≥0.43 mm) as measured by dermal fibrosis (p=0.02).

Conclusions: Our results demonstrate that extent and thickness of regression in thin PCM is significantly associated with adverse clinicopathologic parameters including high Clark level, high Breslow thickness, mitotic figures, ulceration, lymphovascular invasion, vertical growth phase as well as with reduced overall survival. We propose to include regression (both extent and depth of inflammation and fibrosis) as a strong adverse prognostic marker in patients with thin PCM.

491 The Rich Inflammatory Infiltrate in Kaposi Sarcoma Contains Phenotypically Defined Tumor Associated Macrophages with Potential Tumor Immune Suppressor and Angiogenetic Functions

Gianna Ballon, Ethel Cesarman. North Shore LIJ Health System, Lake Success, NY; Weill Cornell Medical College, New York, NY.

Background: Kaposi sarcoma (KS) represents an endothelial cell neoplasm with a rich inflammatory infiltrate of still unclear origin and function. Tumors can secrete several factors in the tumor microenvironment responsible for changes in myeloid differentiation that can favor tumor immune evasion, angiogenesis and tumor progression. M1 toward M2 polarization is favored by increase in IL10 and reduction in IL12, which lead to reduced Th1 activity and tumor immune evasion, along with angiogenesis and tumor promotion. The main myeloid subpopulations responsible for these effects in tumors are tumor associated macrophages (TAM) and myeloid derived suppressor cells (MDSC). Our recent data on transgenic mice expressing vFLIP (a KSHV gene) in endothelial cells showed remodeling of myeloid differentiation with M1 toward M2 polarization and expansion of cells phenotypically identified as MDSC and TAM, suggesting a pathogenetic role for these myeloid cells in KS.

Design: Seven cases of KS were retrieved from the pathology files at Weill Cornell/ New York Presbyterian Hospital. All were shown to be positive for KSHV LANA by immunohistochemistry. These were stained for two macrophage markers, CD163 and CD68 (using a double IHC approach). In a previous study, which evaluated TAM immunohistochemically in neoplastic skin lesion, CD163 was identified as a more abundant, sensitive, and accurate marker of TAM, compared to CD68, demonstrating that CD163+ TAM produce pro-tumorigenic factors and display a M2 phenotype with an important role in tumor immunity. Therefore, we considered CD163 a *bona fide* marker of TAM in our study.

Results: A rich inflammatory infiltrate was found in all KS cases analyzed. All cases showed numerous cells that were singly positive for CD163, while only two cases had in addition many cells that were double positive for both CD163 and CD68. Positivity of CD68 did not correlate with HIV status on this limited cohort. This exclusive expression of CD163 documented drift toward CD163+ TAM phenotype.

Conclusions: Our finding of a preferential to exclusive expression of CD163+ macrophages in KS supports our *in vivo* experimental data that ascribe to the remodeling of myeloid differentiation a key pathogenetic role in Kaposi sarcoma, and provides the rational for dissecting the function of these CD163+ myeloid cells to identified key molecular signatures that can be targeted by specific therapeutic approaches.

492 A Functional In Situ Approach to TILs in Melanoma: A Critique on the Current Morphological Classification

Francesca Bosisio, Jasper Wouters, Nathalie Volders, Marguerite Stas, Joost van den Oord. KUL, Leuven, Belgium; Università degli studi di Milano-Bicocca, Milan, Italy.

Background: Tumor-infiltrating lymphocytes (TILs) are classically divided into "brisk", "non-brisk" and "absent" categories, and this classification bears prognostic significance; in particular the heavy "brisk" category is associated with excellent prognosis, and the "absent" category is associated with thick melanomas. However, little is known about the functional status of TILs or of the antigen-presenting machinery of melanoma cells in these categories, and the prognostic significance of the "non-brisk" category is poorly defined. Nevertheless, the increasing usage of immunomodulatory therapies in disseminated melanoma requires knowledge of the efficacy of the immune response in melanoma.

Design: As immune checkpoint-targeted therapies are given to stage IV patients, 58 melanoma metastases were immunohistochemically stained for MHC machinery molecules (HLA ABC, HLA-DR, b2-microglobulin, TAP1, TAP2), T-cell subsets (CD4, CD8, PD-1) and for signs of interferon-gamma (IFNg) induction (CXCL9 and RT-qPCR for IFNg).

Results: The overall correlation between "brisk" TILs and the presence of signs of IFNg production in the melanoma microenvironment (i.e. CXCL9+ melanoma cells or macrophages) was significant (p: 0.009). Furthermore, "brisk" TILs were consistently associated with overexpression of the MHC machinery molecules on melanoma cells. On the other hand, 22% of melanomas with "non-brisk" TILs showed no obvious signs of IFNg production, indicating considerable heterogeneity in this category. Interestingly, 46% of the melanomas with "absent" TILs had CXCL9+ macrophages in the microenvironment, suggesting an alternative inducible agent.

Conclusions: The "brisk" morphological category of TILs suggests the presence of activated (IFNg-producing) T-cells and the presence of melanoma cells that are well equipped for appropriate antigen expression. On the other hand, the "non-brisk" and "absent" categories represent heterogeneous categories in which the morphology only partially reflects an ongoing immune response. Therefore, further studies have to fine-tune the "non-brisk" category into subsets with ineffective antigen-presentation or with inactive CD8+ T-cells. A thorough functional evaluation of the "non-brisk" and "absent" categories is needed for further stratification of patients in need of immune checkpoint therapy.

493 BRAF Mutation Analysis: A New Tool for Pathologists in Metastatic Melanoma; Multicenter Retrospective Evaluation on 239 Cases in French Private Pathologists Laboratories

Jerome Chetritt, Nicolas Josselin, Alain Gaillot, Claude Deplechain, Emmanuel Watkin, Philippe Chalabreysse, Delphine Raoux, Nicolas Weinbreck. Institut d'Histo Pathologie - IHP, Nantes, France; Sipath, Clermont-Ferrand, France; Cypath, Lyon, France; Medipath, Frejus, France.

Background: BRAF tumor V600 mutation status has to be evaluated with a molecular test for targeted therapy.

In France, such onco-molecular tests are performed in centralised Regional Institutional Molecular Biology Platforms under INCA's control (National Cancer Institute). Time to result and consolidated data are crucial for oncologists.

Through a feasibility study we evaluated our capacity to use in our labs a novel fully automated system which gives BRAF V600 mutation status directly from formalin-fixed paraffin-embedded (FFPE).

Design: Evaluation has been done in 4 major independent centers on 239 metastatic melanoma patients starting from 1st July 2013.

The Idylla™ BRAF Mutation Test[1] has been used in this study. The test consists of a disposable cartridge which contains all reagents for fully integrated sample preparation

and real–time PCR. The test detects the BRAF V600 E/E2/D/K/R/M mutations and takes 90 minutes from insertion of FFPE tissue section into the Cartridge up to reporting final result. FFPE tumor sections were qualified by pathologists.
All Idylla™ results were compared with INCA Platform results where various reference methods (RM) are performed.
[1]Not yet available in the USA or Canada
Results: Comparing the results of both tests on 239 patients only 1 Wild Type (WT) was detected in our study while the RM detected V600K/R/M. On the other hand we reported 7 mutations while no mutation was found with RM: 6 cases showed V600E/E2/D (WT on RM) and 1 V600K/R/M (WT on RM). Discordant results will be analyzed by a 3rd method (ddPCR; results will be shown in final poster). Finally 2 cases were excluded because of a mutation in codon 601 detected by RM which is not present in our test and a 'non-contributory' result on RM detected WT by us
Statistical analysis was performed based on dichotomized results mutation versus no mutation. Overall, positive and negative % agreement was calculated together with 95% lower confidence limits. All agreements are above 90% showing that the routine test is similar to the RM. Finally also a kappa statistic was calculated (0.929) indicating almost perfect agreement between both methods.
Conclusions: Private pathologists can use the Idylla™ BRAF Mutation Test routinely, without need of molecular infrastructure. Results can easily be added to TNM or Breslow, leading to faster results towards the oncologist.

494 A Diagnostic Algorithm for Atypical Spitzoid Tumor: Guidelines for Immunohistochemical and Molecular Assessment

Jeong Hee Cho-Vega. University of Miami Miller School of Medicine, Miami, FL.
Background: Atypical spitzoid tumor (AST) carries striking resemblance, clinically and histopathologically, to Spitz nevus (SN) and spitzoid melanoma (SM). Although AST is a rare entity, it is crucial to determine its malignant potential and predict its clinical behavior. Here, I propose a novel diagnostic algorithm to assess the malignant potentional of ASTs.
Design: This algorithm applies a set of IHC (a dual-color of Ki67/MART-1, p16 ^{Ink4a}, and HMB45), a 5-probes fluorescence in situ hybridization (FISH) covering 6p25, 8q24, 11q13, cent 9, and 9p21, and an array-based comparative genomic hybridization (aCGH). For SNs with histologically and immunohistochemically worrisome features (asymmetry, ulcer, deep dermal mitosis, and high-grade cellular atypia, deep dermal high cell proliferation by Ki67/MART-1, complete loss of p16, and/or complete loss of HMB45), the FISH will be performed. For ASTs with positive FISH for melanoma, a diagnosis of SM will be rendered and aCGH will not be needed. For ASTs with negative or borderline positive FISH, then aCGH assay will be performed: If the aCGH demonstrates melanoma abnormalities, a diagnosis of SM will be rendered. If the aCGH is negative or shows a non-melanoma pattern of chromosomal aberrations, then a diagnosis of "AST without or with a specific aCGH signature" will be rendered.
Results: Six cases with spitzoid tumors were prospectively evaluated. Four of those showed negative FISH and aCGH and were diagnosed as "AST". Two cases showed a positive molecular test; In case 1 (21 years old female with a compound AST on the cheek), FISH was negative but aCGH showed losses of chr 9 and 2p and a gain of 5q (aberrations frequently found in melanomas) and thus a diagnosis of "SM" was rendered. In case 2 (14 years old boy with an ulcerated compound AST on the shoulder), FISH was negative but aCGH revealed losses of pericentromeric Chr 6p, Chr 6q, and 22q (aberrations not known to be typical of melanoma) and the tumor was diagnosed as an "AST" and a re-excision of the prior biopsy site, not too much deeper and wider, was recommended.
Conclusions: Correlation between histological, immunohistochemical, cytogenetic/molecular results and clinical information is an integral part of this diagnostic algorithm for ASTs. I believe that this algorithmic approach will provide a comprehensive diagnostic aid to histological criteria of ASTs in daily Dermatopathology practice and will significantly contribute to improve the diagnosis and prediction of clinical behavior of ASTs.

495 The Expression of BMP-2, Fetuin-B, and MGP in Biopsies of Calciphylaxis

Jonathan Davick, Andrew Patterson, Benjamin Kaffenberger, Alejandro Gru. The University of Virginia, Charlottesville, VA; The Ohio State University, Columbus, OH.
Background: Calciphylaxis, or calcific uremic arteriolopathy is a poorly understood disease with a high mortality rate that is most commonly seen in patients with chronic kidney disease (CKD). Previous studies have suggested that ectopic protein expression in vascular endothelium may play a role in the pathogenesis of calciphylaxis and that immunohistochemical (IHC) staining for these proteins may be of diagnostic utility. In this study, we report the expression of three proteins (BMP-2, Fetuin-B, and MGP) in skin biopsies of patients with calciphylaxis compared to patients with CKD and skin ulcers without calciphylaxis.
Design: The Ohio State University medical records were retrospectively reviewed for patients who had undergone skin biopsies with a clinical suspicion for calciphylaxis. The available formalin-fixed, paraffin-embedded skin biopsies from these patients were collected and stained for BMP-2, Fetuin-B, and MGP using IHC techniques. Each of the 23 biopsies were reviewed for staining in subcutaneous vascular endothelium and given a grade of 1 (negative expression), 2 (moderate, positive staining), or 3 (strong, positive staining). Based on information in the patient's medical record, whether or not each patient had a diagnosis of calciphylaxis was also documented. This was done irrespective of the IHC results. Using a chi-squared test, the expression of the three markers was then compared between patients with and without calciphylaxis.
Results: 23 cases available for immunohistochemical staining were evaluated. 8 of the 23 patients had a diagnosis of calciphylaxis, and the remaining 15 patients had CKD and skin ulcers but no clinical diagnosis of calciphylaxis. Immunohistochemical staining for BMP-2 showed positive staining in 88% (7/8) of the calciphylaxis cases and 40% (6/15) of the non-calciphylaxis cases ($p<0.05$). Fetuin-B staining was positive in 63% (5/8) of calciphylaxis cases and 33% (5/15) of non-calciphylaxis cases ($p=0.17$). MGP staining was positive in 88% (7/8) calciphylaxis cases and 66% (10/15) non-calciphylaxis cases ($p=0.36$).
Conclusions: Cases of calciphylaxis demonstrate increased vascular endothelial expression of BMP-2, Fetuin-B, and MGP by immunohistochemistry when compared to biopsies of skin ulcers from CKD patients without calciphylaxis. The difference in BMP-2 staining between calciphylaxis and non-calciphylaxis patients was statistically significant in our study. Our data suggest that these proteins may be useful as diagnostic markers or therapeutic targets in calciphylaxis.

496 DNA Mismatch Repair Status in Keratoacanthoma: Immunohistochemistry-Based Study of 1353 Tumors from 1067 Patients

Renee Eigsti, Carolyn Rysgaard, Ashlynne Clark, Brian Swick, Andrew M Bellizzi. University of Iowa, Iowa City, IA.
Background: Keratoacanthoma (KA), a common though enigmatic squamous tumor, is characterized by rapid growth followed by spontaneous involution. Muir-Torre syndrome, the combination of sebaceous neoplasm (with or without KA) and internal malignancy, is a phenotypic manifestation of Lynch syndrome (LS). LS is due to germline mutations in DNA mismatch repair (MMR) genes, resulting in loss of expression of cognate protein, detectable by immunohistochemistry (IHC). Although the relationship between sebaceous tumors and MMR deficiency (dMMR) is well-studied, KAs have received little attention. 4 studies, examining in total <100 KAs, reported rates of dMMR from 8-16%. We performed a comprehensive evaluation of MMR status in KA.
Design: Tissue microarrays were constructed from all KAs diagnosed at our institution since 1996 with available paraffin blocks. MMR IHC was performed with antibodies to MLH1, PMS2, MSH2, and MSH6, with stains scored as intact or lost. For tumors that screened abnormal in TMAs, dMMR was confirmed in whole sections. Clinical variables collected for each KA included age, gender, anatomic location, and multiplicity. For dMMR tumors and an age/gender-matched control group of MMR-proficient (pMMR) tumors, detailed personal/family cancer history was obtained.
Results: We screened 1353 tumors from 1067 patients. dMMR was ultimately confirmed in 48 tumors from 46 patients. Patients with dMMR tumors were significantly older (75 vs. 69) ($p=0.0015$), with male predominance in both groups (dMMR, 30M:16F; pMMR, 544M, 477F). dMMR was due to MLH1 deficiency in 74% (34 pts), MSH2 deficiency in 22% (10), and MSH6 deficiency in 4% (2). Of 32 dMMR patients with follow up, 6 (23%) had a history of colon cancer (CRC); in 2 KA preceded CRC. Of 16 evaluable patients, 2 (13%) met Amsterdam Criteria (AC) for LS. In the age/gender-matched control cohort of 92 patients, only 3 (3%) had CRC. Of 69 evaluable controls, none met AC.
Conclusions: In a large, unselected cohort of KAs 4.3% were MMR-deficient. This rate is similar to the frequency of LS in unselected colon and endometrial cancers. CRC was 4x more frequent in this group than expected in the general population. The distribution of MMR abnormalities (MLH1-predominant) is similar to that in Northern European, population-based CRC cohorts and dissimilar to that in endometrial cancer (MSH6-predominant) and sebaceous neoplasms (MSH2-predominant). Given ready availability, IHC-based LS screening in KAs should be considered, and in patients with a family history compelling for LS in which no other tumor is available, testing can be performed on a KA.

497 Multinucleate Cell Angiohistiocytoma: A Study of 5 Cases of an Enigmatic Entity with Further Insights on Its Clinical Presentation

Giovanni Falconieri, Deborah Bonazza, Maurizio Pinamonti, Bostjan Luzar. University of Trieste, Trieste, Italy; University of Ljubljana, Ljubljana, Slovenia.
Background: Multinucleate cell angiohistiocytoma (MCAH) is a benign condition found mostly in the extremities of adult women, presenting as violaceous or erythematous cutaneous nodules characterized by distinct but often subtle histologic diagnostic features. A number of cases have been published in the literature, but data from compiled series suggest that this condition may have a broader clinical spectrum, which in turn implies an expanded spectrum of microscopic diagnoses. We report 5 cases of MCAH, emphasizing their presentation and the initial microscopic interpretation.
Design: Five cases of cutaneous MCAH were retrieved from departmental or consultation files. Clinical features and impression are summarized in table 1.

Sex/ Age	Site	Clinical Presentation	Clinical Impression	Proffered Microscopic Interpretation
M/37	Dorsum of hand	Violaceous plaque, 1 cm	Fibroma	Dermatofibroma
M/47	Knuckles and dorsum of fingers	Multiple papules	Granuloma annulare	MCAH
F/48	Shin	Violaceous plaque, 1.5 cm	Eczema	Dermatofibroma
M/63	Knuckles	Tan, raised 0.8 cm nodule	Basal cell carcinoma, Spitz nevus	Lichen simplex
M/23	Wrist	Tan, raised, 0.4 cm nodule	Spitz nevus	Kaposi sarcoma

Patient ages ranged from 23 to 63 years (median 47); 4 were males, 1 female. Except for 1 case, the preliminary microscopic diagnoses included diverse conditions including

dermatofibroma, lichen simplex, and Kaposi sarcoma. Based on the preliminary diagnosis a panel of antibodies was applied on available tissues against cytokeratins, S100 protein, CD31, CD34, CD68, HHV8, and ER.
Results: All cases were characterized by a dermal haphazard proliferation of venules and capillaries within a variably collagenized ground substance, along with epidermal hyperplasia. Fibrocyte-like elements were recognized along with scattered multinucleate cells harboring hyperchromatic nuclei. The latter cells showed cytoplasmic nuclear bulging. A mild to moderate inflammatory infiltrate was present in two cases. In 3 tested cases, the multinucleate cells were positive for CD68 and negative for all the other markers.
Conclusions: Our data indicate that MCAH is still a frequently underrecognized condition simulating clinically and histologically diverse cutaneous lesions. Although these may be easily ruled out, the histologic distinction from dermatofibroma, lichen simplex or dermal scar may challenge the unexperienced pathologist and requires a high index of suspicion along with proper clinicopathologic correlation.

498 The Generalized Eruptive Keratoacanthoma of Grzybowski: A Reappraisal of a Challenging Conditions Based on 4 New Cases

Giovanni Falconieri, Maurizio Pinamonti, Deborah Bonazza, Joze Pizem, Bostjan Luzar. Trieste University, Trieste, Italy; Ljubljana University, Ljubljana, Slovenia.
Background: Eruptive keratoacanthoma (EKA) is a rare condition characterized by sporadic eruption of numerous follicular papules often associated with intense pruritus and microscopic features comparable to ordinary keratoacanthoma, with less than 50 cases published in the English literature. We report a clinicopathologic study of 4 new cases of EKA.
Design: Cases of EKA were retrieved from departmental files along to clinical information from the referring physicians. In order to be included in the series patients must history of multiple, non-ulcerating cutaneous keratoacanthomas associated with a progressive course and variable systemic symptoms including pruritus.
Results: Four cases of EKA were identified. Salient clinical features are summarized in table 1.

Age/ sex	Salient clinical history	Tumor biopsy site(s)
M/76	Multiple keratotic papules over distal extremities	Shin
M/72	Multiple keratotic papules over both limbs and trunk	Foot, shin
F/56	Prurigo nodularis diffusa lasting for 10 years; keratotic nodules of limbs	Back and limbs
F/74	Multiple eruptions of lower limbs lasting for 21 years	Thigh and leg

Cutaneous lesions presented abruptly as nodules with a central keratotic plug; dramatic, scattered excoriations due to scratching were often present along to scarring (fig. 1).

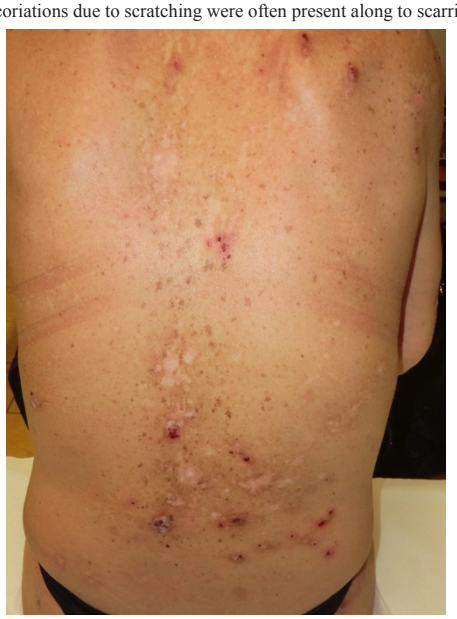

Histologically, florid tumors were comparable to ordinary keratoacanthoma (fig. 1A); features of prurigo nodularis were present as well (fig. 1B).

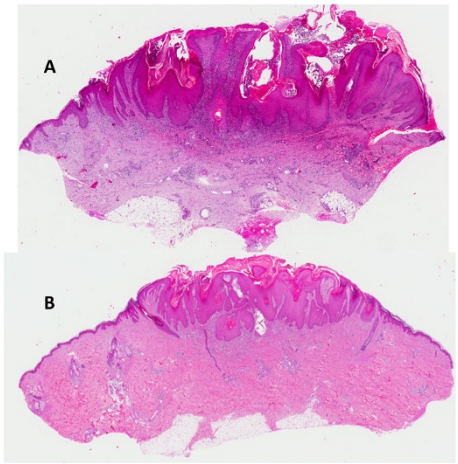

No mucosal lesion was identified.
Conclusions: Our study adds further evidence that EKA affects adult patients with no sex predilection. Due to its dramatic clinical presentation and entailed treatment issues especially pertaining to the control of pruritus, it still poses significant challenges also due to lack of awareness of the condition. Data compilation is probably needed as to set more strict diagnostic criteria for the generalized EKA of Grzybowski

499 Use of a Novel Rabbit Monoclonal Phospho-Histone H3 (Ser10) Versus H&E Mitotic Count in Invasive Melanoma

Regan Fulton, David Altree-Tacha. Phenopath, Seattle, WA; Biocare Medical, Concord, CA.
Background: Mitotic rate is an important prognostic indicator in cutaneous melanoma. It can be difficult to identify mitotic figures (MF) reliably in hematoxylin and eosin (H&E)-stained sections, especially in the context of poor fixation. Recently, a new rabbit monoclonal mitotic marker Phospho-Histone H3 Ser10 (pHH3) was developed and shown to be more specific compared to a rabbit polyclonal pHH3. We investigated the rabbit monoclonal marker pHH3 and compared MF counts with H&E. In a previous study, the authors showed a 243% fold increase in the detection of mitotic activity when using a pHH3 antibody compared to the standard the H&E method.
Design: Eight invasive melanoma cases (whole sections of formalin-fixed paraffin embedded tissues) were randomly selected. Of the 8 cases, 2 cases showed less than optimal fixation. Adjacent sections from each case were cut at 4 microns and were stained with H&E and a commercially available rabbit monoclonal pHH3 [BC39] antibody using immunohistochemistry. Whole slides were examined at 20X with 40X confirmation of equivocal structures. A strict criterion for counting mitoses was employed: condensation of the chromatin, breakdown of the nuclear membrane, and finger-like projections of chromatin. Only tumor cell mitoses were counted, and apoptotic cells were excluded.
Results: Table 1: H&E versus pHH3 Mitotic Counts

Case	Histology Quality	H&E Mitotic Counts	pHH3
1	Good	104	214
2	Good	250	775
3	Good	972	1343
4	Good	122	512
5	Poor Fixation	24	180
6	Good	118	515
7	Poor Fixation	26	185
8	Good	257	344

The 6 cases with good histology demonstrated a total of 1823 mitotic figures by H&E versus 3703 with pHH3, resulting in a 203% increase in MF. In the 2 cases with poor fixation, 50 mitotic figures were identified by H&E versus 265 with pHH3, which represents a 530% increase in the mitotic count. PHH3 examination was more rapid than H&E mitotic cell counting (approximately 50% faster).
Conclusions: Estimating the mitotic rate with rabbit monoclonal pHH3 is more rapid than counting mitotic figures by H&E. pHH3 analysis was faster because less time was required to distinguish positive cells and was much less subjective. Thus, pHH3 staining may be more sensitive and reproducible, especially in cases of poorly fixed tissues.

500 The Expanded Eight-Probe Melanoma Fluorescence In Situ Hybridization (FISH) Assay as an Ancillary Tool in Diagnosing Ambiguous Melanocytic Lesions: An Updated Clinical, Pathological and Cytogenetic Review of 416 Cases

Ruifeng Guo, Kabeer Shah, Lori A Erickson, Thomas Flotte, William R Sukov. Mayo Clinic, Rochester, MN.
Background: Ambiguous melanocytic lesions are diagnostically challenging with uncertain biological behavior. A FISH assay using 4 sets of probes has been used in distinguishing benign nevus from melanoma. Recently four additional FISH probes targeting two new genomic regions were suggested to improve the sensitivity of the FISH assay. Herein we summarize our experience with the expanded FISH panel in analyzing 416 cases of ambiguous melanocytic tumors.

Design: The eight probes used in the expanded melanoma FISH panel targeted chromosomes 6p25 (RREB1), 6q23 (MYB), 11q13 (CCND1), 8q24 (MYC) and 9p21 (CDKN2A), centromeres 6, 8 and 9. The assay was performed and evaluated with the standard published FISH protocol with modifications. 416 cases of diagnostically challenging ambiguous melanocytic lesions submitted for the FISH assay at our institution were analyzed to evaluate the efficacy of the expanded FISH assay.
Results: The differential diagnoses included atypical Spitz nevus(34%), atypical compound nevus (19%), melanocytic tumor of uncertain malignant potential (13%), atypical deep penetrating nevus (9%), atypical cellular blue nevus (3%), and others query melanoma (22%). 92 cases had positive FISH results, with 82 of them subsequently diagnosed as melanomas. Among the 296 cases with negative FISH results, 10 were still diagnosed as melanoma, and the rest had complete excision and optimal surgical margins recommended given the diagnostic uncertainty. 5 melanoma cases were confirmed only by the new probes, either MYC amplification or CDKN2A loss, which therefore increased the assay sensitivity from 83.7% to 89.1 %, while the specificity remained at 96.6%. 28 cases with highly variable final diagnoses ranging from melanoma to atypical compound nevus showed equivocal FISH results, including tetraploidy, polyploidy, and monosomy 9. No recurrence occured in 30 patients with FISH results with short-term follow-up (median 10 months). 7 FISH positive and 2 FISH negative melanoma patients underwent sentinel lymph node biopsies with 50% metastasis rate in either group.
Conclusions: The FISH assay is a relatively sensitive and specific method in classifying ambiguous melanocytic lesions. The addition of the new 4 probes improves the sensitivity of the assay. Diagnostic and clinical uncertainty still remains in cases with equivocal or negative FISH results, which need long-term follow-up for further characterization.

501 Differential Expression of CD123 in Photoallergic Dermatitis, Spongiotic and Lichenoid Dermatoses, and Mycosis Fungoides

Andy C Hsi, Xiaofan Pang, Andras Schaffer. Washington University School of Medicine, St. Louis, MO.
Background: Photoallergic dermatitis is a form of contact dermatitis in which the allergen is activated by light to produce an eczematous eruption. It appears clinically and histologically similar to other types of contact dermatoses, while its clinical management is significantly different. In addition, chronic photoallergic reactions can be morphologically indistinguishable from mycosis fungoides (MF) and some lichenoid dermatoses. Recent studies have suggested that ultraviolet (UV) irradiation induces skin accumulation of plasmacytoid dendritic cells (PDC), which are critical in the pathogenesis of lupus-associated photosensitivity. The role of PDC in photoallergic dermatitis, classical contact and lichenoid dermatoses, and MF is not known. PDC can be identified by its high level of CD123 expression. Knowledge of CD123 expression may help differentiating photoallergic dermatitis from other spongiotic and lichenoid processes as well as MF.
Design: Eight cases of well-documented photoallergic dermatits, 11 non-photoallergic dermatoses (6 classical contact and 5 lichenoid dermatoses), 5 lupus erythematosus (LE), and 17 MF were stained with CD123. The proportion of the CD123+ cells in the total infiltrate and their distribution within the biopsy were analyzed.
Results: The results are summarized in the Table below. Statistically significant differences in the proportion of CD123+ PDC were observed between MF and photoallergic dermatitis (P<0.001), non-photoallergic dermatitis (P<0.001), LE (P=0.003). There were no significant differences between the non-MF categories (P>0.05). Statistical significance was observed in the percentage of cases with CD123+ epidermal clusters between MF and photoallergic dermatitis (P=0.003), non-photoallergic dermatoses (P=0.007), and LE (P=0.011). No significant differences in the presence of epidermal clusters were seen between the non-MF categories (P>0.05).

Diagnosis	Median % CD123+ cells (range)	% of cases with epidermal clusters
MF (n=17)	4.86 (0.18-15.01)	6
Photoallergic dermatitis (n=8)	39.37 (12.61-52.74)	63
Non-photoallergic dermatoses (n=11)	39.53 (14.65-48.91)	55
LE (n=5)	45.75 (13.26-51.03)	60

Conclusions: PDC is present in significant numbers in LE, photoallergic dermatitis, spongiotic and lichenoid dermatoses. CD123 is not a useful marker in differentiating photo-induced processes from other benign dermatoses. In contrast, the proportion of CD123+ cells and the presence of epidermal clusters may be reliable ancillary assays in distinguishing benign dermatoses from MF.

502 Differential Neurofibromin Protein Expression in Desmoplastic Melanoma Subtypes - Implicating NF1 Allelic Loss as a Distinct Genetic Driver?

Alexander Kadokura, Noah Frydenlund, Dominick Leone, Shi Yang, Mai P Hoang, April Deng, Marier Hernandez, Asok Biswas, Rajendra Singh, Meera Mahalingam. BUSM, Boston, MA; MGH, Boston, MA; UMASS Medical School, Worcester, MA; Mt Sinai Hospital, New York, NY; Miraca LS, Newton, MA; Western General Hospital, Edinburgh, Scotland, United Kingdom; VA Consolidated Laboratories, Boston, MA; Carver Coll of Medicine, Iowa City, IA.
Background: Loss of the *NF1* allele, coding for the protein neurofibromin, and polymorphism in the proto-oncogene RET, encoding the glial cell line-derived neurotrophic factor receptor, are purportedly common in desmoplastic melanoma (DM). Neurofibromin regulates MAPK signaling of nerve growth factor (NGF) and our recent experience shows an association between the low-affinity NGF receptor and perineural invasion (PNI) in DM. *In vitro* evidence indicates that RET, which also activates the MAPK pathway, is overexpressed in select *Nf1* knockout mice. DM is categorized into pure (PDM) and mixed (MDM) subtypes which differ in prognosis, implying distinct genetic drivers. Most *NF1* mutations result in a truncated/absent protein, making immunohistochemical screening for neurofibromin a surrogate for *NF1* allelic loss. Using anti-neurofibromin, our aims were to ascertain the incidence of neurofibromin loss in PDM and MDM and to evaluate the relationship between neurofibromin, RET, PNI, and established histopathologic prognosticators.
Design: In this IRB-approved study, archival samples with a diagnosis of DM were retrieved and a total of 59 cases identified as meeting criteria for inclusion in the study (54 cases of non-DM served as controls). Immunohistochemistry was performed for neurofibromin, while RET polymorphism and BRAF mutation status were detected by direct DNA sequencing. P-values were generated using chi-square test.
Results: Overall, neurofibromin loss was more common in DM than non-DM (75 vs. 54%, p=0.02). In DM, significant differences in neurofibromin loss were noted in the following: non-sun exposed (SE) vs. SE sites (92 vs. 65%) and PDM vs. MDM variants (88 vs. 63%). No significant associations were noted with gender, presence of a junctional component, Breslow depth, ulceration, mitoses, host response, RETp, BRAF status, or PNI.
Conclusions: Our findings, implicating loss of the *NF1* allele in the biology of PDM, support the hypothesis that DM subtypes have distinct genetic drivers. Lack of an association with RETp and PNI argue against an interaction between neurofibromin and select neurotrophin receptors. Increased prevalence of neurofibromin loss in DM from non-SE sites suggests that UV radiation is not the dominant mutagen in DM.

503 Subungual Atypical Lentiginous Junctional Melanocytic Proliferation in Children and Adolescents: A Clinicopathologic Study

Sameer Khatri, Min Wang, Aleodor Andea, May P Chan. University of Michigan, Ann Arbor, MI.
Background: While lentigo and melanocytic nevi constitute the majority of subungual pigmented lesions in children, occasional cases show highly atypical lentiginous junctional melanocytic proliferations which are difficult to classify due to the lack of typical nevic architecture and the exceptional rarity of subungual melanoma in the pediatric population. We aimed to characterize the clinical and pathologic features of these rare lesions.
Design: Our pathology database was searched for subungual atypical junctional melanocytic proliferations in patients under 20 years of age. The histologic slides were reviewed to identify cases with a predominantly lentiginous growth pattern. Clinical data was obtained from medical records. Fluorescence in situ hybridization (FISH) targeting RREB1, CCND1, MYB, CDKN2A, +/-MYC was performed on cases with available tissue blocks.
Results: Seven cases were found, including 4 males and 3 females of Asian, Caucasian, and African American descents. The mean age was 8.7 years (range, 2-19 years). All but one lesion were located on the fingers. The mean width of the pigmented streaks was 0.3 cm (range, 0.1 to 0.6 cm). Hutchinson sign was noted in 3 patients. Microscopically, all cases were characterized by ill-defined borders, lentiginous growth, and pagetoid scatter. Five (71%) lesions showed focal or poor nesting. Two (29%) cases had areas of confluence. Six (86%) lesions consisted of both epithelioid and dendritic melanocytes. Nuclear enlargement, angulation, and hyperchromasia were present in 4 (57%), 2 (29%), and 4 (57%) cases, respectively. Prominent nucleoli were observed in 1 (14%) of the cases. Four (57%) lesions were heavily pigmented. All 3 cases tested by FISH lacked numerical aberrations at the probed loci. Follow-up data was available for 6 cases (mean, 7.3 months). Only one lesion recurred after incomplete excision and was subsequently re-excised. No other recurrence or adverse outcome was noted.
Conclusions: Rare subungual melanocytic lesions from the pediatric population do not classify well as nevi histologically. Some of the atypical features such as predominantly lentiginous growth, pagetoid scatter, confluence, and poor circumscription overlap with those typically seen in subungual melanoma in situ in adults. Despite the lack of invasion, the negative FISH studies, and the young age of the patients, the biologic potential of these lesions remains elusive. Complete excision is recommended to avoid recurrence and potential for aggressive behavior.

504 Detection of Somatic Mutations in Secondary Tumors Associated with Nevus Sebaceus by Targeted Next Generation Sequencing

Jong T Kim, Kimberly J Newsom, Wonwoo Shon. University of Florida, Gainesville, FL.
Background: Nevus sebaceus is now known to be associated with mosaic *RAS* mutations. Mutant *RAS* typically functions as a driver oncogene to induce MAPK and PI3K signaling pathway overactivation, which may explain the high prevalence of secondary tumors associated with nevus sebaceus. Although several previous studies were able to confirm the presence of *HRAS* mutations in secondary tumors that arose within nevus sebaceus, no additional genetic abnormalities ("second-hit") have been identified. Prompted by these observations, we performed targeted next generation sequencing to identify additional mutations in secondary tumors associated with nevus sebaceus.
Design: Three secondary tumors including syringocystadenoma papilliferum, sebaceoma, and basal cell carcinoma were selected. Notably, sebaceoma and basal cell carcinoma occurred within the same nevus sebaceus. Next generation sequencing (NGS) was performed using a clinically validated assay on the Ion Torrent Personal Genome Machine (PGM) with the Ion AmpliSeq Cancer Hotspot Panel v2 covering approximately 2,800 COSMIC mutations from 50 oncogenes and tumor suppressor genes (Life Technologies). Data from the PGM were processed initially using the Torrent Suite Software and further analyzed using Genomoncology platform (www.genomoncology.com).

Results: *HRAS* c.37G>C mutation was detected in all secondary tumors. Furthermore, additional *PIK3CA* c.1633G>A mutation was present in the syringocystadenoma papilliferum, whereas the sebaceoma also revealed *TP53* c.916C>T mutation.
Conclusions: Our findings support the *RAS*-dependent genetic pathway and second-hit model for secondary tumor development in nevus sebaceus, but further studies with a larger number of various secondary tumors are necessary to confirm this statement. To our knowledge, *PIK3CA* and *TP53* mutations have not been previously identified in syringocystadenoma papilliferum and sebaceomas, respectively.

505 An Independent Validation of a Gene Expression Signature to Differentiate Malignant Melanoma from Benign Melanocytic Nevi

Hillary Kimbrell, Loren E Clarke, Darl D Flake, Klaus Busam, Clay J Cockerell, Klaus F Helm, Jennifer M McNiff, Jon A Reed, Jaime Tschen, Jinah Kim, Raymond Barnhill, Rosalie Elenitsas, Victor G Prieto, Jonathan Nelson, Kathryn A Kolquist, Krystal Brown, M Bryan Warf, Benjamin B Roa, Richard J Wenstrup. Myriad Genetic Laboratories, Inc., Salt Lake City, UT; Myriad Genetics, Inc., Salt Lake City, UT; Memorial Sloan Kettering Cancer Center, New York, NY; University of Texas, Southwestern Medical Center, Dallas, TX; Penn State Hershey Dermatology, Hershey, PA; Yale Dermatopathology, New Haven, CT; Baylor College of Medicine, Houston, TX; St. Joseph Dermatopathology, Houston, TX; Stanford School of Medicine, Stanford, CA; University of California, Los Angeles, Los Angeles, CA; Curie Institute, Paris, France; MD Anderson, Houston, TX.
Background: Recently, a 23-gene signature was developed to produce a melanoma diagnostic score capable of differentiating malignant and benign melanocytic lesions. The objective of this study was to independently assess the ability of the gene signature to differentiate melanoma from benign nevi in clinically relevant lesions.
Design: A set of 1,400 melanocytic lesions was selected from samples prospectively submitted for gene expression testing at a clinical laboratory. After testing, each sample was subjected to independent histopathologic evaluation by three experienced dermatopathologists. A primary diagnosis (benign or malignant) was assigned to each sample and diagnostic concordance among three dermatopathologists was required for inclusion in analyses. A threshold for minimum tumor volume was established and the sensitivity and specificity were assessed in all tumors that satisfied this threshold.
Results: A threshold melanocytic volume of 10% was established for clinical testing. Excluding the lesions with melanocytic volume below this threshold, the gene expression signature differentiated benign nevi from malignant melanoma with a sensitivity of 91.5% and a specificity of 92.5%.
Conclusions: These results reflect the performance of the gene signature in the diverse array of samples encountered in routine clinical practice.

506 Breaking Bad Dogma: The Diversity of Spindle Cell Lipomas in Women

Jennifer S Ko, Brianne H Daniels, Patrick Emanuel, Vadim Khachaturov, Jesse K McKenney, John R Goldblum, Steven D Billings. Cleveland Clinic, Cleveland, OH; UCSF, San Francisco, CA; Auckland Health Board, Auckland, New Zealand.
Background: Spindle cell lipomas (SCL) are tumors of the upper back/neck (shawl region), and much more common in men (90%). In men, 80% of SCL arise in the shawl region, and those that do not still frequently involve the head and neck. As such, there has been a dogmatic practice of almost exclusively restricting the diagnosis of SCL to this clinical scenario and a hesitancy to diagnose SCL in women. Based on our experience, we hypothesized that SCL in women do not have the same stereotypical presentation as seen in men.
Design: 395 SCL diagnosed at our institution over the last 11 years were analyzed for their clinical and pathologic features. The diagnosis for SCL occurring in women was confirmed at the least via review of H&E stained sections by 2-3 expert pathologists. When material was available, these cases were also analyzed with immunohistochemical (IHC) stains for CD34, desmin, estrogen receptor (ER), and p16. In a subset of cases, *Retinoblastoma1 (Rb)* gene deletion was confirmed with fluorescence in-situ hybridization (FISH).
Results: Of 395 SCLs, 331 (83.8%) occurred in men and 64 (16.2%) occurred in women. Women had a younger median age at diagnosis (52; range 14-83) compared with men (62; range 23-95), p<0.001, t-test. Of the 64 cases of SCL in women, 56 had material available for review (H&E stained slide at minimum). 51/56 were confirmed as SCL; 5 were excluded. SCL in women much more commonly occurred outside the shawl distribution (39/51, 76.5%) compared with men (99/331, 29.9%) (p<0.001), including extremities (17/51, 33.3% versus 32/331, 9.7%; p<0.001) and face (10/51, 19.6% versus 47/331, 14.2%; p<0.05). The cases demonstrated the spectrum of known histologic variants of SCL with varying proportions of: bland spindled cells, ropey collagen, myxoid matrix and mature adipocytes. By immunohistochemistry, 51/51 cases were CD34 positive and 48/48 were desmin negative. Most (33/42) tested cases were negative for ER, and showed loss of p16 expression (29/42), but this was not absolute, even in the 13/14 cases which showed *Rb1* loss by FISH. Three additional cases showed loss of Rb1 by immunohistochemistry.
Conclusions: The conventional dogma of SCL in men does not apply to women. SCL in women have a propensity to occur in unconventional anatomic locations and in a slightly younger patient population. This information should encourage pathologists to include SCL in the differential diagnosis of spindle cell lesions occurring in non-traditional settings.

507 Efficiency of Direct Immunofluorescence Testing: Examination of a Single Institution Experience with Bullous Pemphigoid

Jennifer S Ko, Patrick C Feasel, Steven D Billings. Cleveland Clinic, Cleveland, OH.
Background: Direct immunofluorescence (DIF) panels include antibodies to IgG, IgA, IgM, complement C3, and fibrinogen, and can be ordered prior to H&E slide examination. The rising cost of health care necessitates a more streamlined approach to pathologic diagnoses. Based on our experience, we hypothesized that the preemptive staining of frozen section slides with the standard panel of antibodies for DIF studies is wrought with easily avoided inefficiencies. We have begun our analysis using bullous pemphigoid (BP) as a prototype.
Design: Skin biopsies from within our institution over 5 years (2010-2014) with both DIF and formalin-fixed paraffin-embedded (FFPE) tissue were searched. Cases where bullous pemphigoid was in the clinical differential were selected and analyzed based on the final pathologic diagnosis, results of DIF testing and necessity for DIF testing.
Results: Of 1330 cases with DIF and FFPE tissue, 137 (10%) included BP in the clinical differential. Of these 137 cases, 67 (49%) had positive DIF results, and 90% (60) were bullous pemphigoid. 100% of BP cases were positive for complement C3, and 83% positive for IgG. In DIF-positive BP cases, 35/60 (58%) had quite consistent histologic features and 25/60 (42%) were non-pathopneumonic. 7/67 (10%) of positive cases were non-BP bullous disorders: linear IgA (3), pemphigus vulgaris (2), dermatitis herpetiformis (1), and porphyria cutanea tarda (1), and were positive for IgA or C3 +/- IgG. In one case, DIF was crucial as it identified a clinically unsuspected disease (linear IgA) that could not be diagnosed on H&E stained sections. Within the 137 cases with clinical suspicion for BP, 70 (51%) had negative (47/137, 35%) or non-specific (23/137, 17%) DIF results, and represented primary (24/70, 34%) and secondary (46/70, 66%) bullous disorders. Secondary bullous lesions resulted from spongiotic (39%), hypersensitivity (30%), and other dermatitides (30%). Non-specific DIF findings usually included fibrinogen immunoreactivity. Within the entire cohort, the previously mentioned linear IgA case was the only entirely unexpected finding which necessitated use of antibodies in addition to complement C3 +/or IgG (1/137, 0.75%).
Conclusions: The results of this prototype study strongly support a streamlined approach whereby DIF antibody selection for staining is based upon the disease category and the histologic findings after review of the H&E slide by the pathologist. At the least, our data support the notion that usage of complement C3 and IgA alone is effective for the evaluation of subepidermal bullous disorders.

508 Utility of Whole Genome Single Nucleotide Polymorphism Microarray (SNPM) and Targeted Somatic Mutations in Evaluation of Histologic Mimics of Melanoma

Ravindra Kolhe, Alka Chaubey, Deepa Jagdale, WonSok Lee, Barbara R DuPont, Ashis K Mondal. Georgia Regents University, Augusta, GA; Greenwood Genetic Center, Greenwood, SC.
Background: Majority of the melanocytic lesions can be accurately diagnosed on an adequate biopsy. However, for specific subsets of melanocytic proliferations, there exist conflicting and/or ambiguous features that preclude a definitive consensus diagnosis on histology. In fact, misdiagnosis of melanocytic lesions is at the top of the list of malpractice cases in diagnostic pathology. Currently florescent in-situ hybridization (FISH) testing is utilized to rule out melanoma in these cases but with a very high cut off. Whole genome studies have discovered statically significant oncogenic aberrations in melanoma. The goal of the current study is to investigate the combine utility of SNPM & targeted somatic mutations in melanoma diagnosis.
Design: Fifty cases, on which FISH testing in a reference lab was performed to either confirm/ruled out melanoma were selected for the study. (14 melanoma and 36 histologic mimics of melanoma).

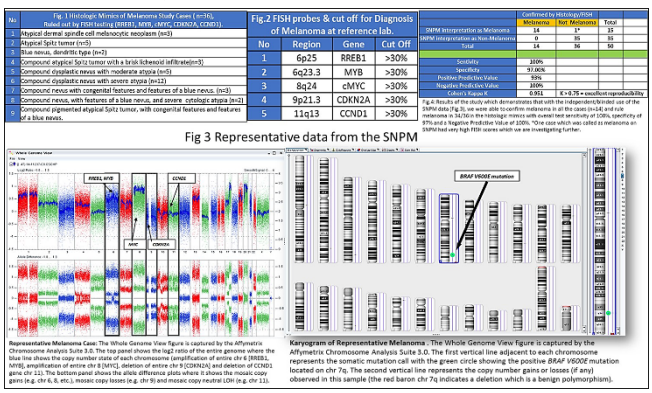

The whole genome SNPM was performed on the DNA isolated from FFPE specimens following manufacturer's protocol & raw data was analyzed in CHAS 3.0 software (OncoScan® assay, Affymetrix, Inc). This platform consist of 274,000 probes including 74 somatic mutations from 9 genes (*BRAF, KRAS, EGFR, IDH1, IDH2, PTEN, PIK3CA, NRAS and TP53*). The diagnosis of melanoma on SNPM was made on the basis of the 5 genomic regions probed for FISH and other statistically significant genomic aberrations seen in melanoma.
Results: With the independent/blinded use of the SNPM data (Fig.3), we were able to confirm melanoma in all the cases (n=14) and rule melanoma in 35/36 of the histologic mimics with overall test Sensitivity of 100%, Specificity of 97% and a

Negative Predictive Value of 100% (Fig.4). In addition it also confirmed the *BRAF V600E* mutation in 8/8 cases and discovered additional mutations in *EGFR, PIK3CA* and *NRAS* genes.
Conclusions: Here for the first time we demonstrate the utility of robust technique for confirming/ruling out melanoma in histologically difficult cases. We anticipate that this approach of obtaining high resolution data from a small FFPE sample at reduced cost, will facilitate in diagnosis of melanoma which was not previously possible.

509 A New FISH Panel and Next Generation Sequencing May Aid in Classifying Atypical Melanocytic Neoplasms

Luke Latario, Kristine M Cornejo, Xun Wu, Melissa McEnery-Stonelake, Xiuling Meng, Keith Tomaszewicz, Ediz F Cosar, April Deng, Lloyd Hutchinson. University of Massachusetts Medical School and UMass Memorial Healthcare, Worcester, MA.
Background: A subset of melanocytic neoplasms are difficult to unequivocally categorize morphologically as benign or malignant and are termed atypical. Melanoma (MM) can be distinguished from benign nevi (BN) on the basis of characteristic chromosomal aberrations and gene mutations. Previously, we identified a fluorescent in situ hybridization (FISH) panel that could distinguish BN from MM with 100% sensitivity and specificity, respectively. In this study, we used our new FISH panel in combination with next generation sequencing (NGS) to determine if a molecular signature consisting of copy number and mutation status can more accurately classify atypical melanocytic neoplasms into benign or malignant categories.
Design: We collected a total of 30 atypical melanocytic neoplasms (atypical spitzoid tumors, n=25; dysplastic nevi, n=5). FISH was performed using an 8 probe panel composed of 2 commercial probe sets (set 1: CCND1, RREB1, CEP6, MYB; set 2: CCND1, RREB1, MYC, 9p21) and our new panel (RREB1, MYC, PTEN, BRAF). A copy number gain or loss was calculated as average counts of >2.5 or <1.5, respectively. Cases with 2 or more abnormalities were considered positive. Protein expression for CCND1, P16, PTEN and MYC were evaluated and correlated with FISH analysis. NGS was performed on a subset of cases (n=17) looking at 50 cancer "hotspot" gene mutations using the Ampliseq Cancer Hotspot Panel v2.
Results: Six of the 30 atypical melanocytic neoplasms produced a positive FISH result. Of the 6 cases, 2 were positive for set 1 (33%), and the same 5 were positive for set 2 and our new panel (83%, each). Relative to the gold standard, probe set 2, our new panel classified an atypical melanocytic neoplasm as malignant with a sensitivity and specificity of 83% and 100%, respectively. Immunohistochemistry was non-contributory and positive for expression in all cases tested except for 1 case with PTEN loss without a concurrent PTEN deletion or mutation. Gene mutations were detected in cases without chromosome abnormalities and included HRAS (5/17; 29%), BRAF (3/17; 18%), NRAS (1/17; 6%), IDH1 (1/17; 6%) and CTNNB1 (1/17; 6%).
Conclusions: Our new FISH panel performs similarly to commercially available probe sets. The addition of mutation analysis may have limited utility in this setting.

510 SOX-10 and DOG1 Expression in Primary Adnexal Tumors and Cutaneous Metastases of Epithelial Origin

Cecilia Lezcano, Jonhan Ho, Raja R Seethala. University of Pittsburgh Medical Center, Pittsburgh, PA.
Background: Classification of cutaneous adnexal tumors and distinction from metastatic carcinomas to the skin are challenging. We and others have noted SOX-10 and DOG1 expression in normal eccrine glands, but their expression in skin adnexal tumors has not been described. We compare the expression of SOX-10 and DOG1 with other markers used to classify skin adnexal tumors and separate them from cutaneous metastases.
Design: 32 primary eccrine and apocrine tumors, and 32 cutaneous metastatic carcinomas, 18 of which were mammary in origin were arrayed in triplicate (1 mm cores) on tissue microarrays (TMA) using a manual arrayer. Immunohistochemical markers used in this study are summarized in Table 1. Percentage and distribution of expression were recorded; positivity was defined by non-random expression in ≥10% of tumor cells. Normal skin and salivary gland were examined as controls.

Marker	Clone	Company	Dilution
SOX-10	BC34	Biocare Medical	predilute
DOG1	1.1	Thermo Scientific	1:50
S100	polyclonal rabbit	Dako	1:500
p40	polyclonal rabbit	Biocare Medical	predilute
p63	4A4	Thermo Scientific	1:200
ER	SP1	Ventana	predilute
AR	AR441	Dako	1:100

Results: In normal skin adnexa, SOX-10 and DOG1 positivity was restricted to the ductal and myoepithelial components of the eccrine secretory coil. 6 cases (1 primary adnexal tumor and 5 metastases) were lost due to core dropout. SOX-10 and DOG1 were positive in 16 and 10 out of 25 eccrine tumors, respectively. Staining was present in both ductal and myoepithelial components of eccrine tumors with a secretory coil phenotype (i.e. chondroid syringoma, cylindroma), while tumors with an acrospiroma phenotype were negative (i.e. hidradenoma). The sensitivity, specificity, and accuracy of single markers in differentiating primary skin adnexal tumors from metastatic carcinomas is summarized in Table 2.

Marker	Sensitivity	Specificity	Accuracy (%)
SOX-10	55	96	74
DOG1	36	59	47
S100	58	96	76
p40	90	100	95
p63	94	96	95
ER	10	48	28
AR	10	56	31

Conclusions: SOX-10 and DOG1 (along with S100) are markers of eccrine secretory coil differentiation. In distinguishing primary tumors from metastases, SOX-10 is specific, but not sensitive in comparison to p63 and p40. DOG1 is neither sensitive nor specific in this context.

511 Melanoma Micronuclei Identification Using Integrative Nuclear Grade Analysis

Ying-Chun Lo, Alexander Baras, Robert W Veltri, Nemanja Rodic. Yale-New Haven Hospital, New Haven, CT; Johns Hopkins University School of Medicine, Baltimore, MD; Yale University School of Medicine, New Haven, CT.
Background: Occasionally it may be a challenge for pathologists to differentiate nuclei in melanocytic nevi from that in cutaneous malignant melanomas. Computer-based nuclear grading features such as nuclear shape, size, and chromatin texture can objectively and accurately identify nuclear grade. Here we exploited one such computer-based analytical technique to learn more about nuclear features of malignant melanomas.
Design: We first set out to determine nuclear parameters that have ability to classify melanocytic nuclei into either benign or malignant category using logistical regression analysis of preset computer-generated nuclear grading features such as nuclear shape, size, and chromatin texture. We then used newly identified features to evaluate nuclear features using conventional microscopy. Fifty patients with either benign melanocytic nevi or cutaneous malignant melanomas were identified in the present cohort. Using 5-micrometer thick Feulgen-stained tissue sections, approximately 85 lesional nuclei were captured and selected in each case using an AutoCyte Image Analysis System (Figure 1). Sixty one different nuclear morphometric descriptors (NMDs) were calculated for each lesional nucleus.
Results: Using logistic regression, the variance of seven NMDs were found to be different between two melanocytic lesion categories ($P < 0.001$)(Figure 1). Amongst these, nuclear membrane variance showed greatest ability to separate melanoma nuclei from the benign counterpart. Using this newfound knowledge we applied conventional microscopy to carefully evaluate melanoma nuclear membranes in Feulgen-stain section (Figure 2). We identified minute micronuclei in close apposition to many primary melanoma nuclei. Matched step sections showed that micronuclei are not easily identifiable in routine H&E sections, but are readily identifiable in Diff-Quik stained cytologic smears.
Conclusions: We identify disruption of the nuclear envelope, specifically formation of micronuclei, as a novel objective morphologic feature of malignant melanomas.

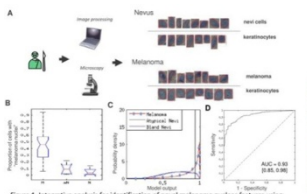

Figure 1. Integrative analysis for identification of novel melanoma nuclear features using both computer-generated nuclear grade classifier, termed nuclear morphometric descriptors (NMDs), and conventional microscopy. (A) Schematic representation of experimental procedure to identify melanoma nuclear features. (B&C) Performance characteristics of selected NMDs feature classifier developed by image analysis and computer-generated nuclear grading. (D) Receiver operating characteristic curve for selected NMDs generated diagnostic sensitivity of 85% and specificity of 98%. High specificity illustrates the ability of NMDs to discriminate melanoma nuclei from those of benign counterpart.

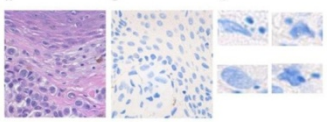

Figure 2. Identification of melanoma micronuclei nuclear using conventional microscopy. (A&B) Representative mid-power photomicrographs showing profiles of vertical growth phase malignant melanoma in routine H&E preparation and Feulgen-stained tissue sections. (C) Representative high-power photomicrographs showing melanoma nuclei in close apposition to primary melanoma nuclei. A&B: Original magnification, 200 X. C: Original magnification 1000 X.

512 Cutaneous Intravascular Epithelioid Haemangioma. A Clinico-Pathological Analysis of 21 Lesions

Bostjan Luzar, Eleni Ieremia, Eduardo Calonje. Medical Faculty University of Ljubljana, Ljubljana, Slovenia; John Radcliffe Hospital, Oxford, United Kingdom; St Thomas's Hospital, London, United Kingdom.
Background: Focal intravascular growth of epithelioid haemangioma (EH) is a well-recognized phenomenon. Nevertheless, data on pure intravascular EHs is lacking.
Design: We analysed a series of cutaneous intravascular EH with special emphasis on their salient clinico-pathological features and correlated them with the disease outcome. To be included in the study, EH had to meet the following criteria: 1) localization in the dermis and/or subcutis and 2) 95% or more of the EH should be within the lumen of the vessel(s).
Results: A total of 21 intravascular EHs occurring in 16 patients were studied (12 males, 4 females, age from 11 to 71 years, mean age 40.2 yrs). The most common presentation was that of a slowly growing asymptomatic mass or nodule (15 of 21, 71.4%). The lesions ranged in size from 2 to 30 mm (mean 13 mm). Solitary lesions by far predominated (13 of 16 patients, 81.2%). Three patients had more than one intravascular EH (3 of 16, 18.8%); two of them within the same anatomical area (ulnar site of the left hand – 3 lesions; right thumb/index finger and forearm – 3 lesions) and one at distant sites (right hand and left finger). Intravascular EHs showed predilection for extremities (13 of 21, 61.9%), followed by head and neck area (8 of 21, 38.1%). The pre-operative duration ranged from 1 to 36 months (mean 8.2). Complete or marginal excision was the treatment of choice in all proliferations. Follow-up was available for 10

of 16 patients (range 4 to 72 months, mean 27.3 months). None of the patients developed local recurrence. On histology, all lesions arose within distended subcutaneous vein(s). They were composed of intraluminal diffuse and lobular proliferation of capillaries, venules and small veins, attached to the vessel wall, and lined by epithelioid endothelial cells. Dispersed among the vascular proliferation was mixed inflammatory cell infiltrate, composed of lymphocytes, plasma cells and eosinophils.

Conclusions: In contrast to classical EH, which typically arises in the head and neck area, intravascular EH shows striking predilection for extremities, in particular hands and fingers. Multifocal occurrence arises either within the same anatomic area, along the path of the affected vein, or at distant anatomical sites. Intravascular growth is not associated with adverse clinical behaviour. Recurrence following complete local excision is unlikely.

513 Gastrin-Releasing Peptide (GRP) and Scleroderma: A Potential Novel Mechanism of Tissue Fibrosis

Elizabeth L McKinnon, Mohamad Ibrahim, Howard Levinson, Mary E Sunday. Duke University Hospital, Durham, NC.

Background: Scleroderma (SSc), a chronic collagen-vascular disease, affects >100,000 Americans yearly. In early stages, patients develop contractures and intradermal fibrosis, often progressing to multiorgan involvement and death. There is no treatment to arrest or reverse the disease process. Recently, a mouse model of SSc was reported, in which bleomycin (Bleo) is injected intradermally for ~21-28 days. Two laboratories showed that reactive oxygen species (ROS) cause this dermal fibrosis. We previously observed that GRP mediates pulmonary fibrotic responses to other ROS sources: hyperoxia or radiation. We now hypothesize that ROS mediate dermal fibrosis via GRP release from cutaneous nerves during ischemia-reperfusion injury from Raynaud's phenomenon, seen in SSc. GRP-positive sensory nerves do mediate itch and neurogenic inflammation. We here test this hypothesis.

Design: 10-week-old C3H/HeJ female mice were injected intradermally on the flank with Bleo (100-µg/day) for 5 days, weekly. Immediately after Bleo, some mice were given the potent antioxidant, N-acetylcysteine (NAC) IP. Other Bleo-injected mice were given GRP blockade IP with mAb 2A11 twice weekly. After 3 weeks, skin specimens were processed for routine histopathology, including Masson's trichrome staining. Dermal thickness was quantified by an observer with no knowledge of mouse identities.

Results: The Bleo mouse model was validated by using dermal thickness as a measure of fibrosis, as widely described. Bleo alone resulted in 39% increase in dermal thickness (using ImageJ), which was completely inhibited by NAC. In one experiment, mice given Bleo+2A11 for GRP blockade had ~50% reduction in dermal thickness with minimal collagen deposition compared to Bleo alone.

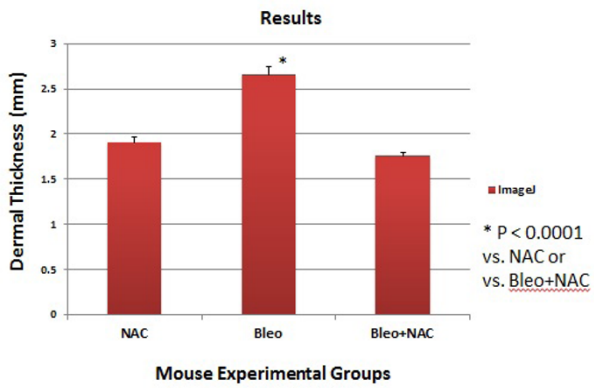

Conclusions: Our study confirms that ROS trigger Bleo-induced dermal fibrosis. In addition, this ROS effect appears to be mediated by GRP. Ongoing studies will evaluate vasculature, nerves, macrophages, markers of ROS and hypoxia, and GRP-related genes. The Bleo mouse model could also clarify how dermal fibrosis results from other ROS sources including radiation, burns, or chronic graft-versus-host-disease. New concepts of SSc pathogenesis could lead to novel therapeutic approaches.

514 Whole Exome Sequence of Merkel Cell Carcinoma Reveals a High Degree of Genomic Instability

Henry McNett, Haley Abel, David Larson, Viveca Bjornhagen, Hong Xie, Weng-Onn Lui, Eric J Duncavage. Washington University, St. Louis, MO; Karolinska Institutet, Stockholm, Sweden.

Background: Merkel cell carcinoma (MCC) is a rare neuroendocrine tumor with an aggressive clinical course that harbors integrated Merkel Cell Polyomavirus (MCPyV) in up to 80% of cases. Compared to other neoplasms, very little is known about the landscape of somatic mutations and clonal architecture of MCC. We sought to determine the somatic mutation rate of MCC in primary tumors and paired metastatic samples.

Design: We identified a set of 11 well-characterized MCC cases including 4 frozen tumor/normal blood pairs and 7 formalin-fixed tumor/metastasis pairs. The average patient age in this series was 77. Whole exome sequencing (WES) was performed on all 22 samples; additional probes were included to cover the MCPyV genome. Cases were sequenced using 2x101bp reads and data were analyzed for a full spectrum of mutations using VarScan2, Samtools, Lumpy, and CopyCAT2.

Results: A mean coverage of 81% of the exome was sequenced to at least 20x in all MCCs. In the 4 paired tumor/normal samples a mean of 660 mutations predicted to alter protein coding were detected. The majority of these variants were C>T transitions, although one case (from the scalp) showed a marked increase in C>A transversions. Among all 11 primary MCCs, the most commonly mutated 'cancer-associated genes' with coding region mutations were TP53, RB1, ATR, and NOTCH1, each mutated in 3/11 cases. CNV analysis demonstrated large (>1Mbase) gains and losses 10/11 cases with a mean of 5.4 CNVs/case. MCPyV viral integration sites were identified in 7 of 11 cases with an average of 2 integration events/case.

Conclusions: Using WES of tumor/normal pairs we demonstrate that the MCC has a high mutation rate, comparable to lung and bladder cancer. The majority of mutations are C>T transitions associated with spontaneous DNA mutations, although we note one case on sun exposed skin with a high number of C>A transversions associated with DNA damage. We further show that nearly all MCCs harbor multiple somatic amplifications and deletions. Together these findings suggest that MCC has a high degree of genomic instability compared to other cancer types.

515 Comparison between myPath-Melanoma Gene Expression Score and Fluorescence In-Situ Hybridization on an Extended Series of Melanocytic Lesions

Eugen C Minca, Rami N Al-Rohil, Min Wang, Jennifer Ko, Victor G Prieto, Michael T Tetzlaff, Steven D Billings, Aleodor Andea. Cleveland Clinic, Cleveland, OH; MD Anderson Cancer Center, The University of Texas, Houston, TX; University of Michigan Medical Center, Ann Arbor, MI.

Background: Melanoma accounts for most skin cancer-related deaths and has an increasing incidence. Accurate diagnosis and distinction from atypical nevi can be difficult using light microscopy alone. Fluorescence in-situ hybridization (FISH) and melanoma gene expression score (myPath, Myriad Genetics) have emerged as ancillary tools to further inform this distinction. No study has attempted to correlate FISH, gene xpression score, consensus histopathologic impression and clinical outcome on a series of challenging melanocytic lesions.

Design: Our study addresses this comparison on 91 formalin-fixed paraffin-embedded skin biopsies collected from three separate institutions and separated into 2 groups: 33 histopathologically unequivocal lesions (13 malignant, 20 benign) and 58 challenging lesions interpreted by expert consensus (22 favor-malignant, 22 favor-benign, 14 ambiguous). Melanoma-FISH was performed using probes for 6p25, 11q13, 8q24 and 9p21/CEP9 and scored according to established criteria. Analysis by myPath gene expression score was performed and interpreted by the manufacturer as "benign", "indeterminate" or "malignant".

Results: In the unequivocal group, melanoma-FISH and myPath score showed 91% and 87% agreement with the histopathologic diagnosis respectively, both with 100% specificity and 83% inter-test agreement. In the challenging group, FISH and myPath score showed 66% and 64% agreement with the histopathologic interpretation respectively, with 74% inter-test agreement. In this group, melanoma-FISH was more sensitive but less specific than gene expression score. The inter-test agreement was 78% overall, excluding indeterminate results. Discordant test results occurred in 17/91 cases from both unequivocal and challenging groups. Discrepancy with the sentinel node status available on a small case subset occurred with both tests.

Conclusions: Melanoma-FISH and gene expression score are valuable ancillary tools, though both have limitations and return discordant results in a subset of cases. Follow-up studies with clinical outcome data, limited in our work, are warranted to establish the accuracy of these tests for the classification of melanocytic lesions.

516 BRAF and Epithelial-Mesenchymal Transition in Primary Cutaneous Melanoma – Insights Provided by Snail and E-Cadherin Expression

Brendon Mitchell, Dominick Leone, John K Feller, Noah Frydenlund, Shi Yang, Meera Mahalingam. University of Florida, College of Medicine, Gainesville, FL; BUSM, 72 E Concord Street, Boston, MA; University of Iowa, Carver College of Medicine, Iowa City, IA; VA Medical center, 1400 VFW PKWY, West Roxbury, MA.

Background: In melanoma cell lines, upregulation of the transcriptional repressor Snail occurs with a concomitant decrease of its target E-cadherin, both hallmarks of epithelial-mesenchymal transition (EMT). To date, this association has not been established *in vivo*.

Design: In this IRB approved project, a total of 68 cases (34 BRAF mutant, 34 BRAF WT) from archival tissue samples with a diagnosis of primary cutaneous malignant melanoma met criteria for inclusion in the study. Immunohistochemistry was performed for Snail and E-cadherin, while BRAF exon 15 mutation status was performed using DNA Sanger sequencing.

To ascertain the clinical correlates of BRAF mutational status, Snail and E-cadherin expression, separate (bivariate analyses) chi-square tests of independence were used if expected cell counts were greater than 5.

Results: Snail expression was demonstrated in 29% of BRAF mutant and 26% of BRAFWT cases (p=NS) and was significantly associated with a greater propensity for ulceration (42% vs. 13%, p=0.02). Vascular invasion was marginally associated with snail in that PCMs with absent expression were less likely to show vascular invasion (89.5% vs. 100% p=0.08). Overall, E-cadherin expression was present in 26% of BRAF mutant and 71% of BRAF WT cases (p=0.0003). Loss of E-cadherin expression was associated with female gender (60% vs. 34% p=0.05), BRAF mutation (74% vs. 29%, p=0.0003), thickness ≥1mm (68% vs. 32%, p=0.004), presence of mitosis (63% vs. 25%, p=0.007), and ulceration (75% vs. 44%, p=0.05). BRAF mutation was associated with male gender (60% vs. 30%, p=0.02), Breslow thickness (p=0.007), thickness ≥1mm (68% vs. 29%, p=0.002), and ulceration (75% vs. 42% p=0.02). Snail expression did not correlate with loss of E-cadherin expression (47% vs. 53%, p=0.79).

Conclusions: Our findings, indicating that mutant BRAF represses E-cadherin expression, implicate a catalytic role for BRAF in EMT. Expression of Snail and repression of E-cadherin are associated with select established adverse histopathologic prognosticators in PCM. Snail may be of potential utility as an adjunct putative therapeutic target in BRAF mutant melanomas.

517 Differential NFAT Expression in Primary Cutaneous CD4+ Small Medium Sized Pleomorphic T Cell Lymphoma and Other Forms of Cutaneous T Cell Lymphoma and Pseudolymphoma

Shabnam Momtahen, Aaron Muhlbauer, Cynthia Magro. Weill Cornell Medical College, New York, NY; Ross School of Medicine, Portsmouth, Dominica.

Background: Primary cutaneous CD4+ small-medium-sized pleomorphic T cell lymphoma (PCSTCL) has emerged as a distinct clinicopathological entity and its potential derivation from a follicular helper T cell has been suggested. Due to a considerable degree of overlap with pseudolymphoma, the diagnosis is challenging. Nuclear factor of activated T cells (NFAT) signaling plays a critical role in T cell activation and nuclear up-regulation of NFAT has been suggested in lymphomagenesis.

Design: 126 cases (61 males, 65 females, mean age=54) including 17 PCSTCL, 45 mycosis fungoides (MF), 5 lymphomatoid papulosis (LyP), 5 anaplastic large cell lymphoma (ALCL), 8 peripheral T cell lymphoma, not otherwise specified (PTLNOS), 12 precursor lesions of MF (i.e. cutaneous T cell dyscrasia) and 34 pseudolymphomas were studied. The number of cells with nuclear stain was counted per 10 HPF. Two-tailed statistical analysis was used for comparison between PCSTCL and all other groups. A *P*-value <0.05 was considered statistically significant.

Results: All cases of PCSTCL showed NFAT nuclear stain (mean=273±220) with no cases exhibiting exclusive cytoplasmic stain (fig.1a). The cells with nuclear stain were larger manifesting a follicular helper T cell phenotype such as positivity for PD1, ICOS, CXCL13 and BCL6. In comparison, a dominant cytoplasmic stain was seen in all cases of MF (fig.1b) with few cases revealing rare nuclear stain, mostly in tumor stage MF (mean=5±8, p=0.0001). All cases of pseudolymphoma showed a dominant cytoplasmic stain with rare nuclear stain (mean=3±8, p=0.0001). No significant difference was seen between MF and pesudolymphoma (p=0.06). ALCL cases showed an almost exclusive cytoplasmic stain (Mean=43±91, p=0.003); similar result was seen in LyP (mean 6±13, p=0.0001). A significant difference was noted between PCSTCL and PTLNOS (mean=16±38, p=0.0001) as well as precursor lesions (mean 3±3, p=0.0001).

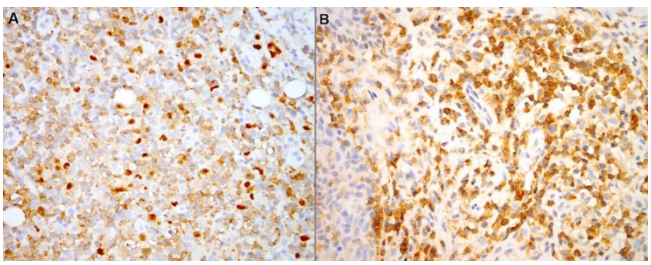

Conclusions: Differential expression of NFAT is a useful marker. When assessing T cell infiltrates where the differential diagnosis is between a PCSTCL versus pseudolymphoma, a significant degree of nuclear staining of lymphocytes could be suggestive of PCSTCL.

518 Cytogenetic Analysis as a Diagnostic Adjunct in Distinguishing the Borderline Melanocytic Tumor from Melanoma

Shabnam Momtahen, Aaron Muhlbauer, James Wang, Cynthia Magro. Weill Cornell Medical College, New York, NY; Ross School of Medicine, Portsmouth, Dominica.

Background: FISH has recently emerged as a technique to better assess the malignant potential of histologically ambiguous melanocytic lesions. However, the usefulness of FISH has not been conclusively established. In this study we further explored the diagnostic value of FISH in distinguishing borderline melanocytic tumors (BMT) from melanoma.

Design: 84 cases of BMT were analyzed between 2010-2015. The BMT groups composed of 2 forms of spitzoid borderline neoplasia represented by the superficial atypical Spitz tumor (AST) and conventional AST of childhood, BMT of the deep penetrating nevus variant (BMTDPN), the pigmented epithelioid melanocytoma (PEM) and borderline nevoid tumor. Probes targeting 5 loci of CCND1 on 11q13, RREB1 on 6p25, MYB on 6q23, CDKN2A on 9p21 and CEP 6 control probe were used. The designation of positive FISH indicated that the criteria were fulfilled to be considered positive for melanoma.

Results: The patients comprised 58 females and 26 males (age range:1-73, mean age:35). Of 6 cases of superficial AST, 1 met the FISH criteria for melanoma and 1 was indeterminate due to polyploidy. In the conventional deeper-seated AST group of childhood, FISH was positive in 7 of 18 cases. Of the 37 cases of borderline nevoid tumors 5 showed positive FISH results and 4 were equivocal due to polyploidy. 4 of 15 of cases of BMTDPN were positive for FISH. Of 2 cases of PEM neither showed positive FISH results. A borderline tumor with overlapping features was favored in 6 cases, while none of them met FISH criteria diagnostic of melanoma.

Conclusions: Although FISH has proven to be highly sensitive and specific in distinguishing unequivocally benign or malignant lesions, however, in cases of ambiguity, these parameters cannot be assessed with great confidence. The 4-probe set (excluding 9p21) consistently showed chromosomal aberrations throughout all groups with 17 of the 84 (20%) of total cases meeting the diagnostic criteria for melanoma. In reviewing those cases the baseline histology was still held to be consistent with a borderline tumor and not diagnostic of melanoma. One would surmise that additional oncogenic events and or other discriminatory cytogenetic abnormalities not disclosed in the limited 4 probe FISH panel are critical in establishing a malignant phenotype. Polyploidy is another inherent limitation, which leads to false positive results due to the absolute signal counts incorrectly reflecting relative imbalances in the tumor genome. Our study evaluated a large number of cases and the clinical follow-up is ongoing.

519 Keratin 17 Expression and Immune Phenotype of Anti-TNF-α Refractory Psoriasis and Anti-TNF-α Related Psoriasiform Dermatitis

Andrea Moy, Mandakolathur Murali, Daniela Kroshinsky, Thomas Horn, Rosalynn Nazarian. Massachusetts General Hospital, Boston, MA.

Background: Th1- and Th17-related cytokines are incriminated in the etiopathogenesis of psoriasis. These cytokines have been shown to upregulate epidermal keratin 17 (K17) expression in psoriasis and, in response, K17 promotes their production. Biologic therapies targeting TNF-α are effective therapeutic agents for psoriasis, although their mechanism of action has not been fully elucidated. Paradoxically, psoriasis may worsen and psoriasiform dermatitis (PsoD) may arise de novo in patients treated with anti-TNF agents for inflammatory disorders.

Design: We investigated epidermal K17 expression and the Th cell immune phenotype in skin biopsies of psoriasis not treated with TNF-α inhibitors (n=9), psoriasis refractory to TNF-α inhibitors (n=11), PsoD related to TNF-α inhibitor treatment (TNFPsoD) (n=9), and atopic dermatitis (n=9). Immunostains for K17, CD3 and dual staining with CD4 and T-bet, GATA-3, or STAT-3 (transcription factors reported to be specific and mutually exclusive for Th1, Th2, and Th17 cells, respectively) were evaluated. Epidermal K17 expression was recorded as present or absent. CD3+ cells and dual-labeled CD4+/T-bet+, CD4+/GATA-3+, and CD4+/STAT-3+ cells were counted and the percent of each Th cell subtype of CD3+ cells was determined.

Results: All cases of refractory psoriasis and TNFPsoD and 10 of 11 (91%) cases of untreated psoriasis showed K17 expression. In comparison, only 2 of 9 (22%) cases of atopic dermatitis had K17 expression (p<0.01). A significant difference in the percent of Th1 and Th17 cells was detected between untreated and refractory psoriasis; refractory psoriasis had fewer Th1 cells (4% vs. 12%; p<0.01) and more Th17 cells (49% vs. 20%; p=0.01). TNFPsoD also showed fewer Th1 cells compared to untreated psoriasis (3% vs. 12%, p<0.01). There was a hierarchy in the Th17/Th2 ratio in refractory psoriasis, TNFPsoD, untreated psoriasis, and atopic dermatitis (0.68 vs. 0.54 vs. 0.41 vs. 0.32, respectively), implicating predominance of Th17 in all psoriasiform disorders studied, as compared to atopic dermatitis.

Conclusions: Anti-TNF-α related mitigation of Th1, upsurge of Th2 and Th17 immune responses, and K17 expression may underlie treatment refractory psoriasis and TNFPsoD. These findings provide novel insight into the mechanism of TNF-α inhibitor treatment, implicating a dominant role of Th17 driven inflammation, and lend support for combined IL-17 and TNF-α inhibition in patients with psoriasis.

520 The Microenvironment in Primary Cutaneous Melanomas: Immunophenotypic Characterization and Evaluation for T Regulatory Cells (Tregs) in a Subset of Tumor Infiltrating T Lymphocytes (TIL) Associated with Primary Melanocytic Tumor Regression

Kumaran Mudaliar, Arielle Gray, Solomiya Grushchak, Michael I Nishimura, Stephanie Kliethermes, Kyle Carey, Kelli A Hutchens. Loyola University Chicago, Maywood, IL.

Background: Areas of spontaneous tumor regression can be seen in the absence of therapeutic intervention, both clinically and histologically in over 25% of primary cutaneous melanomas at initial diagnosis. A unique subset of T lymphocytes found in regressing melanomas can be histologically distinguished from tumor infiltrating T lymphocytes (TIL) found in areas of tumor progression. We call this unique subset of T lymphocytes regression associated T lymphocytes (RATs). In this study our goal is to use immunohistochemistry (IHC) to determine the phenotype of RATs and TIL in the same biopsy specimen. We also compare the density of T regulatory cells (Tregs) surrounding RATs to that of TIL in primary cutaneous melanoma to determine if immune suppression might be a driving force in determining the local immune reactivity of RATs and TIL.

Design: 14 cases of primary cutaneous melanomas with confirmed areas of progression and regression were collected from archival tissue. Single IHC staining using the Leica Bond III protocol was used to determine absolute CD4+ and CD8+ counts. Double-staining combinations FOXP3+(red)/CD4+(brown) and FOXP3+(red)/CD25+(brown) were performed to identify Treg densities. Treg densities were determined by taking a ratio of the obtained counts per total CD4+ cells. Two independent observers manually counted 3 high-powered 40x fields.

Results: We did not observe a predominance of CD4+ or CD8+ T lymphocytes in either RATs or TIL, however TIL trended toward CD8+ predominance (p = 0.19). There was a significantly lower density of Tregs in RATs compared to TIL when using the FOXP3+/CD4+ Treg marker (p = 0.04) and a marginal difference when using our second, confirmatory Treg marker, FOXP3+/CD25+ (p = 0.11). There was no observable difference between the Treg marker densities (FOXP3+/CD4+ vs. FOXP3+/CD25+) in RATs (p = 0.45), however there was a difference observed in TIL (p = 0.03).

Conclusions: We demonstrated a difference in the tumor suppressive microenvironments surrounding RATs and TIL, with RATs having a significantly lower density of Treg cells. Our data suggests that the absence of an immune suppressive microenvironment is associated with local tumor regression. Further exploration of the tumor microenvironment, including evaluation of myeloid derived suppressor cells and local cytokine expression, is needed to better understand what factors permit local immune destruction of invasive tumor cells.

521 Blood Staging in Mycosis Fungoides

William Munday, Chris Tormey, Alexa Siddon. Yale School of Medicine, New Haven, CT.

Background: In 2010, the American Joint Committee on Cancer (AJCC) incorporated blood staging into the TNM classification in mycosis fungoides (MF) . Since this revision, blood flow cytometry has become routine in MF patients regardless of stage. Interestingly, the staging modification was based on MF patients with tumor (T3) or erythrodermic (T4) stage disease. The relevance of blood staging in patients with plaque stage (T1/T2) disease is therefore unknown. Here we address the utility of blood staging

in MF patients with plaque stage skin disease (T1/T2), and those suspected of plaque stage disease. Further, we propose a scoring system to determine when blood staging should be performed based on clinical and histologic features.
Design: Blood flow cytometry from 59 patients evaluated for MF were retrieved from our database over a five-year period. Blood involvement was considered positive if any of the following were detected: abnormal immunophenotype of CD4+ population; CD4/CD8 ratio >10 and CD3 absolute count high; CD4/CD8 ratio >10 and CD4 absolute count high; CD4 absolute count high and CD4+CD7- >40%; CD4 absolute count high and CD4+CD26- >30%. Skin biopsies were available in all cases. Histologic features were assigned a point value: epidermotropism without spongiosis =1pt;, lymphoid nuclear atypia =1pt. Clinical features: (T3/4)=4 pts; lymphadenopathy=1pt; non-sun exposed site=1 pt; age >70 = 1pt.
Results: Average patient age 70 years. Six patients had positive flow cytometry (ave. age = 77 yrs); four presented with erythrodermic stage (T4) disease; each scored greater than or equal to 4 points. One patient with a positive result had plaque stage (T1/T2) disease; this patient also scored 4 points. One patient with a positive flow result had a score less than 4 points (on follow up, no diagnosis of MF). A score greater than or equal to 4 points had a positive predictive value of 63% for blood involvement by MF. A score less than 4 had a negative predictive value of 98%.
Conclusions: Our results suggest that MF patients with blood involvement are largely restricted to high stage cutaneous disease (T3/T4). The detection of blood involvement in patients with plaque stage disease (T1/T2) is likely of little significance. The proposed scoring system also provides a mechanism for determining which patients require blood staging (score greater than or equal to 4 qualify for blood staging).

522 Proposal of a New Molecular Classification of Sebaceous Carcinoma with Its Clinical Significance

Hee-Young Na, Ji Eun Kim, Ji-Young Choe, Ji Yun Yun, Sun-ah Shin, Ho-Kyung Choung, Min Joung Lee. Seoul National University Hospital, Seoul, Republic of Korea; Seoul Municipal Governmet-Seoul National University Boramae Hospital, Seoul, Republic of Korea; Seoul National University Bundang Hospital, Seoul, Republic of Korea; Hallym University Sacred Hospital, Anyang, Republic of Korea; Seoul Municipal Government-Seoul National University Boramae Hospital, Seoul, Republic of Korea.
Background: Recent studies revealed presence of sex hormonal receptors and extracopies of HER2 gene in a subset of sebaceous carcinoma, raising high possibility of common pathogenesis between sebaceous carcinoma and breast carcinoma. Herein, we proposed a novel molecular classification system adapted from that of breast carcinoma, and evaluated its clinical significance.
Design: Thirty seven cases of sebaceous carcinoma were recruited from three university hospitals in Korea. Review of histopathology with immunohistochemistry (IHC) for ER, PR, AR, CK5/6, Ki67 and fluorescence in situ hybridization (FISH) for HER2 gene was performed in all cases.
Results: Most cases occurred in the eyelid (30) with localized diseases (26) but progression was found in eleven; six with recurrence, five with regional or distant metastasis. IHC for ER, PR and AR showed positivity in 14 (37.8%), 10 (27.0%), and 23 (62.2%) cases, respectively. Grade 2 or more of HER2 positivity was found in 10 of 37 (27.0%). HER2 gene amplification was observed in two (5.4%) cases, all grade 3 HER2 IHC. CK5/6 was positive in 11 (29.7%) cases. According to our classification, 13 cases belonged to luminal-1, 4 to luminal-2 in the ER or PR positive groups. In ER and PR negative groups, there were 6 HER2, 8 all-negative, and 6 core basal types. Extraocular tumor showed significantly higher CK 5/6 positivity. Expression of PR was associated with longer progression free survival with marginal significance (p=0.052). Molecular classification showed a significant prognostic value with the best overall survival for the luminal 2 subtype and the worst for all-negative phenotype.
Conclusions: This is the first study to divide sebaceous carcinoma into 5 categories based on the IHC profile and find its clinical significance. This study will offer new insight about providing targeted therapy in intractable cases of sebaceous carcinoma.

523 Melanomas of the Vulva: A Retrospective Analysis of Clinical and Histopathologic Parameters in 40 Patients

Priyadharsini Nagarajan, Jonathan L Curry, Jing Ning, Jin Piao, Phyu P Aung, Doina Ivan, Carlos A Torres-Cabala, Victor G Prieto, Anais Malpica, Michael T Tetzlaff. The University of Texas MD Anderson Cancer Center, Houston, TX.
Background: Vulvar melanomas are uncommon, constituting 4-10% of all vulvar malignancies. It remains controversial if conventional parameters predictive of outcome also apply to these tumors—owing to their relative rarity. Here, we analyze the association between histopathologic prognostic parameters and measures of outcome.
Design: We identified 40 patients with primary vulvar melanomas. Demographic, anatomic, histopathologic features, time of diagnosis, recurrence, metastasis and death were recorded. The probabilities of disease specific survival (DSS) from diagnosis were estimated using Kaplan-Meier methods. Univariate Cox proportional hazards regression models were used to assess the association between the recorded characteristics and DSS.
Results: Of the 40 patients (range: 20 to 83 years, median:53.5 years), 33 (83%) were Caucasians and melanoma primarily involved the labia in 29 (73%) and the clitoris in 11 (28%). Mean tumor thickness was 3.79 mm (range: 0.3-35.0mm). 18% were thin melanomas (pT1, tumor thickness ≤1.0mm), and 30% were pT4 (tumor thickness >4.0mm). Dermal mitotic figures were identified in 65% of cases (mean=5/mm^2). Ulceration, lymphovascular invasion (LVI), regression and perineural invasion (PNI) were present in 55%, 30%, 18% and 13%, respectively. Twenty six of 40 patients (65%) died due to vulvar melanoma; 10 (25%) were alive at last follow up; and 4 (10%) died due to other causes. The median DSS from diagnosis was 79.2 months and the 3-year survival rate was 70% (95% CI, 56.2%-85.3%). Univariate Cox regression analysis demonstrated the following associations with decreased DSS: (i) tumor thickness >2.0mm (HR=6.23, p<0.01), (ii) ulceration (HR=3.02, p<0.01), (iii) dermal mitotic figures (HR=4.56, p=0.01), (iv) LVI (HR=4.05, p<0.01) and (v) microscopic satellitosis (HR=17.91, p<0.01). Metastasis was associated with a poor outcome (HR=12.55, p<0.01). In addition, older age also correlated with reduced DSS (HR=1.05, p<0.01). Other parameters such as anatomic location (clitoral involvement), regression, PNI, status of (sentinel) lymph node and surgical margins did not correlate significantly with survival in this study.
Conclusions: Older age at diagnosis, tumor thickness (>2.0mm), presence of ulceration, dermal mitotic figures, LVI, microscopic satellitosis, metastasis correlate with reduced disease specific survival, supporting that conventional histopathologic parameters are also predictive of outcomes in vulvar melanoma.

524 BRAF Profiling and Testing in an Irish Population

Odharnaith O'Brien, Sandra Murphy, Linda Feeley, Derek Power, Cynthia Heffron. Cork University Hospital, Cork, Ireland.
Background: The assessment of BRAF gene status is now standard practice in patients diagnosed with metastatic melanoma with 40 - 60% of melanomas possessing a BRAF mutation. It is an important predictive factor, with its presence predicting a clinical response to treatment with BRAF inhibitors. The gold standard in determining BRAF status is currently by DNA-based methods (PCR, etc). More recently, a BRAF V600E antibody has been developed which may be of use as an alternative to molecular testing.
Design: We assessed the incidence of BRAF mutation in our cohort, as determined by PCR, as well as looking at clinical and histopathological features of our BRAF mutated versus non mutated populations. We also investigated the sensitivity and specificity of the anti-BRAF V600E VE1 clone antibody in detecting the presence of the BRAF V600E mutation. An initial cohort of 132 cases from patients diagnosed with metastatic melanoma, and whose BRAF mutation status had been determined previously by PCR testing, was identified. Of this cohort, 122 cases were suitable for testing with the BRAF V600E VE1 antibody clone. Formalin fixed paraffin embedded tissue samples from each patient were stained and assessed by blinded observers.
Results: The incidence of BRAF mutation in our cohort, as assessed by PCR, was 28.8% (38/132). Patients with the BRAF mutation were found be significantly younger at age of diagnosis with BRAF mutated melanomas having a tendency to being thinner, more mitotically active as well as more likely to be of superficially spreading subtyep. The antibody showed a sensitivity of 86.1% with a specificity of 96.88%. The positive predictive value was 96.9%; the negative predictive value was 94.4%. The concordance rate between PCR and immunohistochemical BRAF status was 95.1% (116/122). One false positive case and five false negative cases were observed.
Conclusions: Interestingly, the rate of BRAF mutation in our cohort (28.8%) was lower than international published rates of 40 - 60%. This may reflect ethnic or geographic differences within population cohorts. The high concordance rate of PCR and immunohistochemical (IHC) methods in determining a patient's BRAF status suggests that antibody testing is a viable, cost effective, alternative to PCR testing. The BRAF V600E VE1 antibody clone would be suitable as a screening test for the BRAF mutation. Cases of metastatic malignant melanoma should be stained initially by IHC with all negative cases being subsequently submitted for PCR testing to identify variant BRAF mutations not detected by IHC.

525 The Utility of Immunohistochemical and Histological Features to Distinguish between Erythema Multiforme and Cutaneous Graft Versus Host Disease

Stephanie Petkiewicz, April Deng, Patrick O'Donnell, Kristine M Cornejo. University of Massachusetts, Worcester, MA.
Background: The distinction between graft versus host disease (GVHD) and erythema multiforme (EM) challenges both clinicians and pathologists. Post-transplant patients are on multiple drugs making EM just as likely as GVHD. Histologically, both conditions show basal vacuolization, apoptotic keratinocytes and intraepithelial and superficial perivascular inflammatory infiltrates. The presence or absence of eosinophils alone is not a reliable way to distinguish between the two entities. We have attempted to determine histological and immunohistochemical features which may be helpful in making a specific diagnosis.
Design: Eighteen cases of GVHD and 19 cases of EM were selected from pathology archives. Hematoxylin and eosin stained slides were generated and all cases were immunohistochemically stained with CD20, CD3, CD4, CD8 and CD123. The presence of positively stained cells in the epithelial and the dermal compartments was assessed. Approximate percentages of the inflammatory infiltrate comprised of CD4 and CD8 was determined for both intraepidermal and dermal compartments. P values were calculated using Fisher's Exact test.
Results: EM cases more commonly had a heavier dermal inflammatory infiltrate than GVHD cases (p<0.0001) and were more often associated with the presence of eosinophils (p=0.0019). There was no difference in the density of the epidermal inflammation. CD3 staining highlighted prominent lymphocytic infiltrates in both epidermal and dermal compartments, comprising the majority of the inflammatory cells. A larger percentage of the dermal cells was CD4 positive in EM (p=0.0391). GVHD more often had a denser dermal CD8 content but this was not significant (p=0.0991). EM had a higher percentage of CD20 positive cells in the dermal infiltrate (p=0.0029). Staining with CD123 was non-contributory.
Conclusions: The histological distinction between GVHD and EM is a challenge for pathologists. We have determined histological and immunohistochemical features that may be helpful in making a specific diagnosis. EM has a heavier dermal infiltrate with more CD20 and CD4 positive cells and more eosinophils than GVHD, which were all significant. Using these features, the pathologist should be able to more confidently render a definitive diagnosis.

526 Relationship between p53 Status and Clinicopathologic Variables in Cutaneous Basal Cell Carcinoma

Kevin A Pettit, John VanBuren, Brian Swick, Andrew M Bellizzi. University of Iowa, Iowa City, IA.

Background: Basal cell carcinoma (BCC) of the skin is the most common malignancy in whites. Cases predominate on sun-exposed sites. Although rarely metastasizing, they may be locally destructive. Clinical aggression can be predicted based on factors including histologic subtype (morpheaform and infiltrative variants), anatomic site (head and neck), and size. Given an etiologic relationship with UV-radiation, frequent p53 inactivation is not surprising, although published rates have varied. We performed a "molecular-based" assessment of p53 immunohistochemistry (IHC), accounting for patterns associated with missense and null mutations, as well as physiologic p53 accumulation. We hypothesized that p53 status would correlate with clinicopathologic variables, especially morphologic subtype and anatomic site.

Design: We assembled a large cohort of BCCs of the following subtypes: nodular, superficial, infiltrative, micronodular, and morpheaform. For each, we recorded age, gender, and anatomic site. p53 IHC (clone DO-7) was scored as wild-type (weak to moderate staining), missense-mutation (clonal areas of diffuse, strong staining), or null (clonal areas of completely absent staining) pattern; rarely a combination of patterns was observed in a single tumor. The p53 result could be dichotomized as wild-type vs. abnormal. The chi-square test of association was used to compare p53 status vs. clinicopathologic variables, with $p<0.05$ considered significant.

Results: We assessed 287 cases (average age 63, 150M:137F) of the following subtypes: nodular (n=72), superficial (65), infiltrative (59), micronodular (55), and morpheaform (36). 63% of tumors occurred on the head and neck, while only 4 (1.4%) occurred on non-sun-exposed sites. Overall, 45.3% of cases were p53 abnormal, including 50% (2/4) on non-sun-exposed sites (these cases were excluded from further statistical evaluation). p53 null only represented 5% of abnormals. p53 status was significantly associated with histologic subtype ($p<0.001$), with superficial (61%) and micronodular (24%) tumors most and least likely to be p53 abnormal. p53 was also significantly associated with anatomic site ($p<0.001$), with upper extremity (86%) and head and neck (38%) tumors most and least likely to be p53 abnormal. p53 status was not significantly associated with age or gender.

Conclusions: p53 inactivation is common in BCCs, although it varies significantly based on histologic subtype and anatomic site. Given ready availability, p53 IHC status could be incorporated into models predicting disease recurrence. Use of our "molecular-based" interpretative approach is recommended.

527 New Markers for the Recognition of Primary Cutaneous CD8-Positive Epidermotropic Cytotoxic T-cell Lymphoma

Steliana F Racean, Emma Linares, Carmen Gonzalez-Vela, Santiago Montes, Susana Armesto, Pablo Gonzalvo, M Asun Gonzalez-Moran, Victor Alegre, Sonia Alonso, Javier Freire, Manuela Mollejo, Miguel Angel Piris. University Hospital Marqués de Valdecilla, Santander, Spain; Hospital Cabueñes, Gijón, Spain; University Hospital León, León, Spain; University Hospital General de Valencia, Valencia, Spain; University Hospital Elda, Elda, Spain; Hospital Virgen de la Salud, Toledo, Spain.

Background: Primary cutaneous CD8-positive aggressive epidermotropic cytotoxic T-cell lymphoma (CD8-AECTCL) constitutes less than 1% of all cutaneous T-cell lymphomas (CTCLs). It is considered a provisional entity according to the WHO classification with no definite diagnostic criteria. This tumor has a distinctive clinical presentation and aggressive clinical course, without a standard therapy and represents a diagnostic and therapeutic challenge. Histological recognition of CD8 T cells neoplasm, including CD8-positive Mycosis Fungoides and type D Lymphomatoid papulosis is a difficult task and require clinical assessment.

Our hypothesis is that CD8-AECTCL is a separate entity that may be recognised using histological analysis and immunohistochemical markers.

Design: We analyze a series of 12 CD8-positive epidermotropic CTCLs (6 CD8-AECTCL and 6 other CD8-positive cutaneous T-cell lymphomas). Cases were obtained from Marqués de Valdecilla Department of Pathology. Clinical information of the patients was collected, including age, sex, clinical manifestations, follow-up (months) and local recurrence. Immunohistochemical analysis was performed against CD3, CD4, CD8, CD30, TCRbetaf1, TCR gamma, TIA-1, Granzime B, Perforin, pSTAT3 and NFATC1, according to manufactures protocols. Chi square distribution was analysed using GraphPad 6 suite.

Results: CD8-AECTCLs had a clinical behaviour more aggressive that others CD8-positive epidermotropic CTCLs, with a mortality rate of 50% within a period of 32 months of following. None of the other CD8-positive cutaneous T-cell lymphomas patients died of disease.

The expression of NFATc1 in CD8-AECTCL showed significant differences ($p = 0.0209$) when compared with the other CD8- positive cutaneous T-cell lymphomas. Analysis of pSTAT3 expression showed a significant trend ($p = 0.1213$). The other molecular markers showed no difference between the different entities.

Conclusions: A diagnosis of CD8-AECTCL should be based on a combination of clinical, histopathology and immunohistochemical findings. Our data suggest that the expression of NFATc1 or pSTAT3 in CD8-AECTCL could be a differential marker for this disease, allowing diagnosis and facilitating specific treatment.

528 Comprehensive Genomic Profiling of Cutaneous Merkel Cell Carcinoma

Aseeb Rehman, Mark Bailey, Siraj M Ali, Julia A Elvin, Jo-Anne Vergilio, James Suh, Ling Gao, Sara Shalin, David M Jones, J Andrew Carslon, Martin C Mihm, Vincent A Miller, Philip J Stephens, Jeffrey S Ross. Albany Medical College, Albany, NY; Foundation Medicine Inc., Cambridge, MA; University of Arkansas Medical Systems, Little Rock, AR; Brigham and Women's Hospital and Harvard Medical School, Boston, MA.

Background: Merkel cell carcinoma (MCC) is a rare, highly aggressive neuroendocrine (NE) malignancy of skin and soft tissue associated with the MCC polyoma virus infection. We used comprehensive genomic profiling to search for clinically relevant genomic alterations (CRGA) that could potentially lead to targeted therapies for patients with clinically advanced MCC.

Design: From a series of 26,602 clinical samples, DNA was extracted from 40 microns of FFPE sections from 72 consecutive cases of relapsed and locally aggressive MCC. CGP was performed on hybridization-captured, adaptor ligation based libraries to a mean coverage depth of 540X for 315 cancer-related genes plus 37 introns from 14 genes frequently rearranged in cancer. Genomic alterations (GA) included base substitutions (SUB), INDELs, copy number alterations (CNA) and fusions/rearrangements. Clinically relevant GA (CRGA) were defined as GA linked to drugs on the market or under evaluation in mechanism driven clinical trials.

Results: There were 63 (88%) male and 9 (12%) female patients with a mean age of 67.4 years (range 40-88 years). All tumors were at an advanced clinical stage (either stage III or IV) at the time of sequencing. The primary MCC of skin or soft tissue was used for sequencing in 31 (43%) and a metastatic lesion in 41 MCC (57%). There was a total of 315 GA with a median of 4.38 GA per tumor. 84% of GA were base substitutions, 6% indels, 6% amplifications, 2% deletions and 2% rearrangements. There were 86 CRGA with a median of 1.19 CRGA per tumor. Two (3%) of MCC were HPV16 positive. Testing for MCC polyoma virus was not performed in this study. The most frequent GA involved *TP53* (47%), *RB1* (39%), *NOTCH1* (22%), *MLL2* (15%), *FAT1* (14%), *PIK3CA* and *TERT* (13%), *SPTA1* (11%), *ASXL1*, *LRP1B* and *NOTCH2* (8%) and *PTEN*, *APC* and *ATM* (7%). MCC featured a low frequency of CRGA of 1.11 CRGA per tumor. Biologic pathways of potential for use of targeted therapies included the MTOR and cell cycle regulatory pathways.

Conclusions: Although MCC features GA typical of NE differentiation such as mutations in *RB1*, it has a lower frequency of overall and clinically relevant GA than seen in other NE tumors. Nonetheless, a variety of potential therapy targets for patients with relapsed and metastatic MCC can be identified by CGP that show potential to improve outcomes for patients with this aggressive form of malignancy.

529 ALK-1 Expression in Metastatic Melanoma: Potential for a Therapeutic Target

Kabeer Shah, Justin Moser, Aaron S Mansfield, Lori A Erickson, Thomas Flotte. Mayo Clinic, Rochester, MN.

Background: Malignant melanoma (MM) is an aggressive tumor in need of better treatment options. Immunohistochemical (IHC) expression of anaplastic lymphoma kinase 1 (ALK-1), a receptor tyrosine kinase, has been described in solid and hematolymphoid malignancies with therapeutic significance. We studied a large series of MM to determine the frequency of ALK-1 expression for potential targeted therapies.

Design: 173 MM specimens from 158 patients (114M, 44F; mean age 56.7 years; range 16-91 years; primary sites include 24.2% head and neck, 26.1% trunk, 11.1% upper extremity, 17.7% lower extremity, 4.6% from anogential and mucosal sites, 16.3% unknown) with Stage III disease were utilized for the study. Clinicopathologic and follow up (mean 5.6 years; range 0.2-22.8 years) data were collected from all patients. The included cases were placed on a tissue microarray and stained by H&E and ALK-1 IHC. IHC results were categorized as positive or negative, defined by presence of cytoplasmic staining, and compared by Wilcoxson rank sum test.

Results: 13 cases (7.5%) were identified with ALK-1 positivity (9M, 4F; mean age 53.7 years, range 31-78 years). 2 cases strongly and diffusely expressed ALK-1, while 11 cases revealed variable intensity. One patient expressed ALK-1 within an inguinal lymph node while a subsequent dissection was negative.

The ALK-1 positive cases were identified only in MM from sun exposed primaries (primary sites: 2/36 head, 3/40 trunk, and 3/27 lower extremity, 5/25 unknown). The 8 specimens from anogenital and mucosal primaries were negative for ALK-1. When comparing ALK-1 positive cases to ALK-1 negative cases, there were lower mean Breslow depths (2.1 mm versus 4.1 mm), lower mean mitotic counts (4.25/mm^2 and 6.6/mm^2), and less frequent ulceration (14% versus 45%) respectively. 8/13 ALK-1 positive cases had subsequent disease relapse at follow-up. Of the ALK-1 positive patients who subsequently developed widely metastatic disease (n=8), none showed predilection to a particular metastatic site. Overall survival was not statistically significant between the ALK-1 positive and negative cases (10.1 and 5.6 year median survival, p=0.85).

Conclusions: ALK-1 expression was detected in a subset of sun-exposed MM cases (7.5%). Diffuse and patchy cytoplasmic staining is expressed within tumor, potentially representing tumor heterogeneity. Further studies are required to determine the significance of ALK-1 expression. ALK-1 positivity within MM may afford another therapeutic target for this aggressive disease.

530 Clinical Significance of BRAF V600E Mutational Status in Capsular Nevi of Sentinel Lymph Nodes in Patients with Primary Cutaneous Melanoma

Alan E Siroy, Carlos A Torres-Cabala, Michael T Tetzlaff, Priyadharsini Nagarajan, Denai R Milton, Jonathan L Curry, Victor G Prieto, Phyu P Aung. The University of Texas - MD Anderson Cancer Center, Houston, TX.

Background: Capsular nevi (CN) are clusters of benign melanocytes in the capsule of lymph nodes. CN have been previously shown to occur in up to 20% of lymphadenectomy specimens. Previous studies have examined the immunohistochemical (IHC) profile of CN as well as survival data in the setting of melanoma patients with CN in sentinel lymph nodes (SLN). However, the molecular characteristics of CN in relation to prognostic parameters in primary cutaneous melanoma (PCM) patients have not been previously investigated. We assessed the *BRAF* V600E mutation status of CN in the SLN of PCM patients and correlated the CN molecular findings to the clinical, histopathologic, and molecular features of the associated melanoma samples.

Design: A retrospective analysis was performed on 78 CN identified in the SLN of patients with PCM, seen at our institution between 1/2009-2/2015. CN were tested for the presence of *BRAF* V600E mutation by IHC and the results were correlated with the histopathologic and molecular features of the patient's primary melanoma, along with demographic and clinical outcome parameters, including lymph node involvement by metastatic melanoma.

Results: Of the 78 CN assessed, 36 CN (46%) were positive for *BRAF* V600E on IHC. Among these *BRAF* V600E-positive CN, 53% (19/36) were from patients with ≥ stage II melanoma, whereas 62% of the *BRAF* negative cases (26/42) were from stage I melanoma patients (p=0.013). Additionally, a higher percentage of *BRAF* V600E-positive CN cases had metastatic melanoma involving the same lymph node basin (33%; 12/36) in comparison to *BRAF*-negative CN cases (14%; 6/42) (near-significance; p=0.056). *BRAF* mutation status in CN was not significantly associated with other parameters including patient demographics, histopathologic features of the PCM, or the *BRAF* V600E mutation status of the PCM.

Conclusions: A high percentage of CN identified in the SLN of patients with PCM harbor *BRAF* V600E mutation by IHC. *BRAF* mutation status was found to be significantly associated with adverse clinicopathologic parameters, specifically increased tumor stage and lymph node metastasis. This intriguing association warrants further research to elucidate whether BRAF V600E IHC in CN of SLN can be used as a surrogate adverse predictive marker in patients with melanoma.

531 Histopathologic Comparison of Epidermotropic/Dermal Metastatic Melanoma and Primary Nodular Melanoma

Stephanie L Skala, Douglas R Fullen, David P Arps, May P Chan. University of Michigan, Ann Arbor, MI.

Background: Distinction of metastatic and primary melanoma is crucial, as therapy and prognosis differ widely. Metastatic melanoma involving the epidermis and/or upper dermis is particularly problematic due to significant histologic overlap with primary nodular melanoma (PNM). We sought to perform a comprehensive histopathologic analysis of epidermal/dermal metastatic melanoma (EDMM) and PNM, and to determine the most helpful features in differentiating the two.

Design: Our pathology database was searched for EDMM and PNM from 2000-2015. The final diagnoses were confirmed by clinicopathologic correlation. The cases were reviewed by 2 dermatopathologists and 1 pathology resident for various histopathologic features. The obtained data were analyzed by Chi square and t tests between groups.

Results: Seventy-eight EDMM (comprising 70 epidermotropic and 8 upper dermal metastases) and 80 PNM cases were included. Distinguishing features reaching statistical significance are:

	PNM (n=80)	EDMM (n=78)	p-value
Ulcer	39 (49%)	9 (12%)	<0.0001
Exophytic polypoid growth	15 (19%)	1 (1%)	0.0006
Plaque-like growth	3 (4%)	14 (18%)	0.0066
Involvement of adnexal epithelium	22 (28%)	38 (49%)	0.0301
Lichenoid inflammation	14 (18%)	3 (4%)	0.0088
Epimdermal collaretttes	55 (69%)	21 (27%)	0.0002
Tumor-infiltrating plasma cells	26 (33%)	3 (4%)	<0.0001
Regression	26 (33%)	8 (10%)	0.0025
Necrosis	16 (20%)	4 (5%)	0.0083
Associated nevus	9 (11%)	2 (3%)	0.0403
Mitotic rate (mean/medium/range)	12.8/10.0/1-53	5.3/2.5/0-27	<0.0001

Other features including "shoulder", lentiginous growth, intraepidermal nests, pagetoid spread, involvement of preserved rete ridges, pseudoepitheliomatous hyperplasia, expansion of papillary dermis, infiltrative borders, sheet-like growth, pseudomaturation, brisk tumor-infiltrating lymphocytes (TILs), lymphovascular invasion, perineural invasion, and melanosis did not show significant associations.

Conclusions: Multiple histopathologic features are useful in the differential diagnosis of EDMM and PNM. Of these, ulceration and tumor-infiltrating plasma cells (both associated with PNM) are the strongest discriminators of the two groups. Mitotic rate is also significantly higher in PNM than EDMM, although its practical utility is limited by the wide range observed in each group. Contrary to common belief, involvement of adnexal epithelium is more associated with EDMM than PNM, and the presence of brisk TILs does not help in the distinction of the two.

532 The "Pseudoangiomatous" Variant of Spindle Cell Lipoma Is Genuinely "Lymphangiomatous"

Toyohiro Tada, Takashi Tsuchida, Satoshi Baba, Hisashi Tateyama. Toyokawa City Hospital, Toyokawa, Japan; Hamamatsu Medical University, Hamamatsu, Japan; Kasugai City Hospital, Kasugai, Japan.

Background: Spindle cell lipomas (SCL) sometimes show a "pseudoangiomatous" pattern, characterized by irregular branching spaces with villiform projections of fibrocollagenous stroma. Although the spaces were originally interpreted as being created by nonvascular prominent myxoid changes ("pseudoangiomatous"), recently a study reported lining by flat monolayer cells immunohistochemically positive for D2-40 and CD34, suggesting lymphatic nature.

Design: The aim here was to determine whether branching spaces of pseudoangiomatous SCL (PASCL) are truly lymphatic focusing on three cases of PASCL retrieved from surgical pathology files at our hospitals. Immunohistochemical nature of the spaces was investigated using antibodies for PROX1 (lymphatic endothelial marker), ERG, D2-40, CD31, CD34, STAT6, desmin, aSM actin, CD10, and S-100 protein.

Results: All the PASCLs were in subcutaneous tissue, one (case 1) coexisting with "low-fat" features, and were composed of bland uniform spindle cells with short stubby nuclei and eosinophilic coarse ("ropy") collagen bundles, admixed with mature adipocytes, abundant capillary blood vessels, and mast cells. The spindle cells showed uniformly immuno-positivity for CFD34, BCL-2 and CD10, but were negative for STAT6, aSM actin, desmin, and S-100 protein, supporting the diagnosis of SCL. Immunoexpression of D2-40, CD34, CD31 on the monolayer flat cells lining irregular branching thin-walled spaces was variably positive, as shown in Table 1. However, PROX1 and ERG were diffusely positive through the spaces irrespective of parts of the tumor, even on the lining cells negative for D2-40, CD34, and CD31. From these results, the branching spaces can be considered composed of cells with lymphatic endothelial phenotype.

Conclusions: Irregularly branching spaces in so-called "PASCL" are truly lymphatic channels warranting the term "lymphangiomatous SCL."

Case No.	PROX1 (% positive areas)	ERG (% positive areas)	D2-40 (% positive areas)	CD34 (% positive areas)	CD31 (% positive areas)
1	+ (100)	+ (100)	+ (100)	+ (100)	+ (100)
2	+ (100)	+ (100)	+ (20)	+ (20)	+ (20)
3	+ (100)	+ (100)	+ (10)	+ (10)	+ (10)

533 Expression of Melanocytic Immunohistochemical Markers in Melanophages: A Comparison across Platforms

Char-Loo Tan, Priyanka Maheshwari, Yiong-Huak Chan, Shoa-Nian Choo, Siok-Bian Ng. National University Health System, Singapore, Singapore; National University of Singapore, Singapore, Singapore.

Background: The differentiation between malignant melanocytes versus melanophages (MP) can be challenging, especially since MP can coexpress melanocytic markers, albeit uncommonly. In this study, we aim to systematically analyze the immunohistochemical (IHC) expression of 4 commercially available melanocytic markers (HMB45, Melan A, MiFT and SOX10) in order to determine if these markers can reliably distinguish between MP and malignant melanoma (MM). We also tested all 4 markers using both Ventana and Leica autostainers to detect if there is any difference in expression between the 2 platforms.

Design: 30 cases of dermatopathic lymphadenopathy and 6 cases of cutaneous pigmentary incontinence containing MP, and 10 cases of MM were stained for HMB45, Melan A, SOX10 and MiTF using Ventana Ultra and Leica BondIII autostainers. Positive expression is defined as ≥1 cell showing cytoplasmic (HMB45 and Melan A) or nuclear expression (MiFT and SOX10).

Results: For cases containing MP (n=36): Melan A, HMB45 and MiFT were positive in 100%, 94%, 6% of cases using the Ventana compared to 0%, 11%, and 47%, respectively, using Leica system. Notably, SOX10 was negative in 100% of cases using both Ventana and Leica autostainers.

	Ventana		Leica		Discordance rate(%), p-value
N=36	Positive, n (%)	Negative, n (%)	Positive, n (%)	Negative, n (%)	
MelanA	36 (100)	0 (0)	0 (0)	36 (100)	100%, P<0.001
HMB45	34 (94)	2 (6)	4 (11)	32 (89)	83.3%, P<0.001
MiTF	2 (6)	34 (94)	17 (47)	19 (53)	41.7%, P=0.003
SOX10	0 (0)	36 (100)	0 (0)	36 (100)	0%, p=1.0

For MM cases (n=10): Melan A, HMB45, MiFT and SOX10 were positive in 100%, 100%, 80% and 100% using Ventana and 90%, 100%, 100%, 100% using Leica autostainers, respectively. There is no significant discordance (p>0.1).

Conclusions: 1. MP can be positive for melanocytic markers including Melan A, HMB45, and MiFT. The use of these markers can result in diagnostic pitfall in the distinction of MP vs metastatic MM in sentinel lymph node and in cases of dermatopathic lymphadenopathy with melanin deposition.

2. SOX10 is the only marker that can reliably distinguish between MP and MM.

3. The enhanced detection systems in recent models of autostainers may result in the detection of low-level expression of melanocytic markers in MP, which is not previously reported. Pathologists must be aware that the Ventana and Leica autostainers have different detection sensitivity for Melan A, HMB45, and MiFT.

534 Whole Exome Sequencing of 409 Cancer Associated Genes Demonstrates Frequent Clinically Actionable Mutations in Sebaceous Carcinoma

Michael T Tetzlaff, Rajesh Singh, Elena G Seviour, Jonathan L Curry, Diana Bell, Russell Broaddus, Prahlad Ram, Victor G Prieto, Rajyalakshmi Luthra, Bita Esmaeli. University of Texas MD Anderson Cancer Center, Houston, TX.

Background: Ocular sebaceous carcinoma is an aggressive malignancy with frequent local recurrence and metastasis. Surgery remains mainstay treatment but effective systemic therapies for metastatic disease are lacking in part because the molecular alterations driving SC remain poorly understood.

Design: Paired tumor and germline DNA from 27 SC (including 18 primary ocular sebaceous carcinoma (POSC), 5 metastatic ocular sebaceous carcinoma (MOSC) and 4 primary extra-ocular SCs (PEOSC) from 20 patients (7 men and 13 women) were subjected to whole exome next generation sequencing of 409 cancer associated genes (Ion Proton). Ninety-nine genes on the panel are considered actionable (genes for which a matched genotype selected trial exists at our institution). Mutations from different groups were subjected to systematic pathway analyses.

Results: Overall, 9/20 (45%) patients had ≥1 mutation in a clinically actionable gene. In POSC, 81 mutations were identified (median: 3/case; range: 0-16)—12 (15%) of which were clinically actionable from 6/16 (37.5%) patients. In MOSC, 58 mutations were identified (Median: 8/case; range: 2-23)—13 (22%) of which were clinically actionable in 2/3 (66%) patients. The most common mutations among OSC patients included *TP53* (n=9), *RB* (n=7), *PIK3CA* (n=2), *PTEN* (n=2), and *ERBB2* (n=2) and *NF1* (n=2). Systematic pathway analyses demonstrate convergence of these to activation of the PI3K-signalling cascade in OSC, and immunohistochemical studies confirm PI3K pathway activation (increased pAKT and its target pPRAS40) in OSC. A greater number of mutations were identified in PEOSC: a total of 77 from 4 patients (Median: 22.5/case; range: 3-29). These were mostly non-overlapping from OSC (no *TP53* or *RB* mutations were observed in PEOSC). The higher mutational load in PEOSC is attributed to an MSI phenotype in 3/4 patients. Finally, 75% PEOSC patients had ≥1 mutation in a clinically actionable gene, including *BTK*, *FGFR2*, *PDGFRB*, *HRAS*, and *NF1*.

Conclusions: The identification of clinically actionable mutations in 45% patients with SC underscores the potential of clinical next generation sequencing to identify patients who might benefit from a genotype matched targeted therapy. In particular, the frequent activation of PI3K signaling pathways provides a strong rationale for the application of AKT or mTOR inhibitors in the treatment of SC.

535 The Composition, Density, and Location of Immune Infiltrates Correlate with Survival in Merkel Cell Carcinoma

Michael T Tetzlaff, Laurence Feldmeyer, Genevieve R Lyons, Jonathan L Curry, Phyu P Aung, Priyadharsini Nagarajan, Doina Ivan, Carlos A Torres-Cabala, Roland L Bassett, Jennifer A Wargo, Victor G Prieto. University of Texas MD Anderson Cancer Center, Houston, TX.

Background: Merkel cell carcinoma (MCC) is an aggressive cancer with frequent metastasis and death, but few effective therapeutic agents available. Immune checkpoint blockade mobilizes anti-tumoral immunity and has proven effective in a variety of tumors. There is thus a strong rationale to define the density, composition and distribution of immune infiltrates in MCC to determine whether any of these impact clinical outcome and could thus be reasonably leveraged in treatment strategies.

Design: Whole tissue immune profiling was performed for CD3, CD8, PD-1, PD-L1 and MCC polyoma virus T-antigen (MCPv) on 62 primary MCC with annotated clinical outcomes. Automated image analysis of scanned slides (Aperio) quantified immune cell density/mm^2 at the hot spot (HS; 1 mm^2), periphery and tumor center (up to 5 mm^2 each). Associations between covariates of interest and survival were assessed using univariate Cox proportional hazard models. For immune infiltrates, hazard ratios (HR) were calculated per 100 positive cells/mm^2.

Results: Sixty-two MCC (39 MCPv+ and 23 MCPv-) from 45 men and 17 women with a median age 71y (range: 32-91y) were studied. Among clinical-pathologic variables, only perineural invasion correlated with a risk of metastasis to any site (HR: 25.8; p=0.034), but no significant correlation was observed between clinical-pathologic variables and overall survival (OS). Among the four markers interrogated at each location, only an increasing density of CD3+ (HR: 0.92; p=0.0029) and CD8+ (HR: 0.90; p=0.044) T-cells *specifically at the tumor periphery* correlated with improved OS. This effect was also evident among MCPv+ MCC for both CD3+ (HR: 0.92; p=0.023) and CD8+ (HR: 0.83; p=0.035) T-cells *at the tumor periphery*, indicating that for every 100 cell/mm2 increase of either CD3+ or CD8+ T-cells at the periphery of MCPv+ MCC, there was an 8% and 17% reduction in the risk of death, respectively. A similar effect was not observed in MCPv- MCCs. Also, between MCPv+ and MCPv- patients in our cohort, there was neither a significant difference in OS nor any significant differences in the relative immune infiltrates between MCPv+ and MCPV- MCCs, except an increased density of PD-L1+ cells (HS and periphery; p=0.0002) in the MCPV+ tumors.

Conclusions: The density and composition of T-cells at the periphery/leading edge of the tumor is a robust predictor of OS in MCC, especially among MCPv+ tumors. These data provide a mechanistic framework to support the application of immune checkpoint blockade to augment this biologic effect in the treatment of patients with MCC.

536 Nuclear TFE3 Immunoreactivity Is Present in Angiomatoid Fibrous Histiocytomas but Not in Other Cutaneous Histiocytomas

Dianne Torrence, Karen Fritchie, John D Reith, William R Sukov, Wonwoo Shon. University of Florida College of Medicine, Gainesville, FL; Mayo Clinic, Rochester, MN.

Background: TFE3 is one of four members of the microphthalmia-associated transcription factor family and presumably acts as a regulator of many other genes. Angiomatoid fibrous histiocytoma (AFH) is a rare mesenchymal tumor of uncertain lineage harboring specific fusion genes. Interestingly, a previous transcriptional profiling study has also documented high transcript levels of *TFE3* in *EWSR1-CREB1*-positive AFH. For this reason, we evaluated TFE3 protein expression in AFH and other cutaneous histiocytic lesions included in its differential diagnosis.

Design: A total of 14 AFH were retrieved from our surgical pathology archives. Cases were selected based on the original diagnosis, and H&E-stained sections and available fluorescence in situ hybridization (FISH) performed at the time of diagnosis were reviewed to confirm these findings. For comparison, sections from 11 benign fibrous histiocytomas (6 aneurysmal, 3 conventional, and 2 cellular), 3 solitary xanthogranulomas, 2 atypical fibrous histiocytomas, and 2 reactive histiocytic infiltrates were retrieved. Immunohistochemical studies were performed using an antibody directed against TFE3 (MRQ-37, pre-diluted, Ventana, Tucson). Nuclear immunoreactivity was scored as negative (<5%), 1+ (5-25%), 2+ (26-50%), and 3+ (>51%). 3 selected AFH were also analyzed by FISH for *TFE3* gene rearrangement.

Results: Among the cases of AFH evaluated, 13/14 (93%) were positive for TFE3 (3+ in 11 cases, 2+ in 1 case, and 1+ in 1 case). One case showed only rare TFE3 immunoreactivity (<5%); of note, this particular tumor was negative for both *EWSR1* and *FUS* rearrangement by FISH. TFE3 expression was not noted in any cases of fibrous histiocytomas, solitary xanthogranulomas, and reactive histiocytic infiltrate. In one solitary xanthogranuloma, a relatively uniform nuclear TFE3 positivity was also seen in the scattered Touton-type giant cells, whereas the lesional cells were completely negative. Finally, 3 TFE3-positive AFH were negative for *TFE3* gene rearrangement.

Conclusions: In this study, we have shown consistent nuclear TFE3 immunoreactivity in AFH. The exact mechanism of TFE3 protein overexpression in angiomatoid fibrous histiocytomas is unclear at this point. Although larger confirmatory studies are needed, there may be some role for TFE3 immunohistochemistry in the distinction between angiomatoid fibrous histocytomas and other histiocytic lesions.

537 Comparison of Genomic Abnormalities and Gene Expression Analysis in Atypical, Ambiguous and Malignant Melanocytic Lesions

Grace Wang, Min Wang, Ahmed Alomari, Aleodor Andea. University of Michigan, Ann Arbor, MI.

Background: Diagnostic challenge exists in subsets of melanocytic lesions in which conventional histologic assessment is insufficient to reliably distinguish melanoma from nevi. In recent decades ancillary cytogenetic testing based on identifying copy number abnormalities (CNA) using array comparative genomic hybridization/single nucleotide polymorphism (aCGH/SNP) and fluorescence in situ hybridization (FISH) have been developed to aid in the diagnosis of these ambiguous melanocytic lesions. A new molecular test was developed in which melanomas are distinguished from benign nevi with 90% sensitivity and 91% specificity based on the differential expression of 14 genes of interest and 9 housekeeping genes. Our goal is to compare the results of this test with that of aCGH/SNP on a cohort of histologically atypical, ambiguous and malignant melanocytic lesions.

Design: 35 melanocytic lesions including 6 atypical nevi (3 atypical deep penetrating nevi, 2 atypical blue nevi and 1 atypical Spitz nevus), 5 melanomas (3 nodular, 1 superficial spreading and 1 nevoid) and 25 histologically ambiguous lesions were selected (11 atypical Spitz tumors, 11 melanocytic tumors of uncertain malignant potential and 2 BAP1- lesions). Representative tumor areas with sufficient purity were identified on H&E and the corresponding areas were micro dissected. Following DNA extraction array aCGH/SNP was performed using the OncoScan V3 kit from Affymetrix (Santa Clara CA). Cases with more than 1 CNA or a CNA in a region commonly affected in melanoma were regarded as positive. In addition following RNA extraction the gene expression levels of each case were determined by quantitative reverse transcription polymerase chain reaction (qRT-PCR) and was scored with values <-2.1, -2 to -0.1, and >0 interpreted as benign, indeterminate and malignant, respectively.

Results: Results are in table. A good correlation was noted in the atypical nevus and melanoma group. The highest rate of discrepant results was seen in atypical Spitz tumors (82% of cases).

Cases (N)	% aSNP positive	% qRT-PCR malignant	% qRT-PCR indeterminate
Atypical nevi (6)	16.7	0	0
Ambiguous (24)	54.2	8.3	12.5
Melanoma (5)	100	80	20

Conclusions: Concordance between aCGH/SNP and qRT-PCR is good toward the ends of the benign and malignant histologic spectrum. In histologically ambiguous lesions and especially atypical Spitz tumors there is a higher rate of discordant results. Correlation with outcome data is needed to assess the significance of these findings.

538 Clinicopathologic Characterization of Rare Newly Described Follicular Helper T-Cell Variant of Primary Cutaneous T-Cell Lymphoma

James Wang, Giang H Nguyen, Shabnam Montahen, Cynthia Magro. Weill Cornell MC, New York, NY; University of Colorado Anschutz, Aurora, CO.

Background: A recently described variant of peripheral T-cell lymphoma, with 13 reported cases, is characterized by a non-epidermotropic periadnexal/perivascular atypical T-lymphocytic infiltrate presenting as plaques and nodules. The phenotypic profile suggestive of follicular helper T-cell origin (Tfh) is based on variable positivity for Bcl-6, ICOS, CXCL13, and PD1.

Design: Three patient biopsies sent to our institution were held to represent a Tfh variant of peripheral T-cell lymphoma. We obtained clinical history and photographs and performed a literature review.

Results: Our patients were males age 22-70 years who acutely developed violaceous nodules and plaques without constitutional symptoms. One patient had a solitary lesion while two had multiple. One patient had a waxing/waning course for 6 years with cutaneous progression and transient lymphadenopathy, the second had 2 years of disease and incomplete regression despite therapy, and the third had resolution of his solitary lesion with surgical excision.

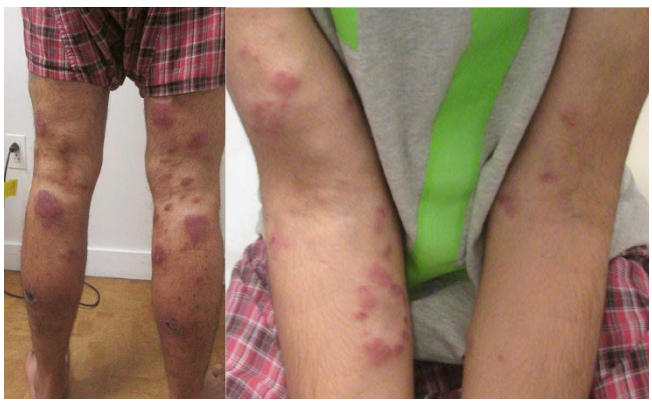

Histological analysis showed a pan-dermal perivascular/adnexal infiltrate of mostly atypical small/medium-sized lymphocytes with accompanying granulomatous inflammation. In one case, large atypical CD30- cells exceeded 30% of the infiltrate. A minority but distinct cell subset was positive for PD1, Bcl-6, ICOS, and CXCL13, indicating Tfh origin. There was significant nuclear expression of TOX and NFAT, two markers known to be upregulated in Tfh cell nuclei.

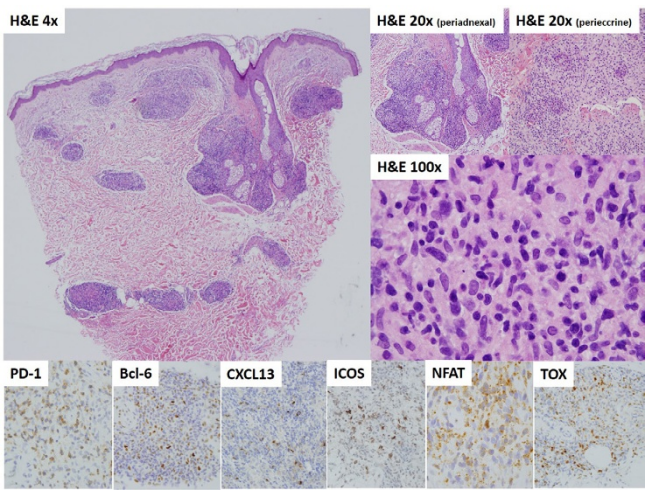

Conclusions: Cutaneous Tfh lymphoma has a characteristic staining pattern in which a subset of infiltrate is positive for Tfh markers. We show that nuclear NFAT and CXCL13 positivity may be useful markers for identifying this lymphoma. In our series, the overall behavior appears to be relatively indolent although complete regression without relapse does not occur except in cases of solitary lesions.

539 Chilblain Lupus Eythematosus Versus Idiopathic Perniosis: Comparative Analysis of Histopathologic Features and CD123 and CD30 Immunostaining

Michael Wang, May P Chan. University of Michigan, Ann Arbor, MI.

Background: Perniosis may be idiopathic (idiopathic perniosis, IP) or associated with lupus erythematosus (chilblain lupus erythematosus, CLE). Recognition of CLE is important as it may herald an undetected connective tissue disease. Previous comparative studies of CLE and IP have shown variable results. More recently, elevated CD123+ plasmacytoid dendritic cells (PDCs) and CD30+ T cells have been described in the cutaneous lesions and the serum of lupus patients, respectively, possibly related to the pathogenesis and progression of the disease. We aimed to compare the histopathologic and immunohistochemical features of CLE and IP in order to identify any useful discriminators.

Design: Our pathology database was searched for "pernio" and "chilblain" from 2000-2015. The cases were classified based on clinical and laboratory data obtained from medical records. H&E slides were examined in a blinded manner for various histopathologic features. CD123 and CD30 immunostains were performed and the proportions of positive cells were estimated in a semiquantitative fashion. The presence of any clusters of >15 CD123+ cells was noted. The data were compared by Chi-square tests between groups.

Results: Twenty CLE and 39 IP cases were included. Interstitial fibrin and moderate to abundant dermal mucin were associated with CLE (p=0.0352 and p=0.0002, respectively). All other histopathologic features examined--perieccrine and perineural lymphocytic infiltrates, lymphocyte karyorrhexis, thrombi or fibrinoid vessels, papillary dermal edema, extravasated red cells, lymphocyte exocytosis, basal vacuolation, necrotic keratinocytes, thickened basement membrane, perieccrine adventitial mucin, and ischemic epidermis--did not reach statistical significance. No significant difference was detected in the percentages of CD123+ PDCs, CD123+ clusters, or number of CD30+ lymphocytes between the two groups.

Conclusions: To our knowledge, this is the largest series comparing the pathologic features of CLE and IP to date. Our data show that histologic discrimination of the two conditions remains a challenge. Of the exhaustive list of features examined, only interstitial fibrin and moderate to abundant dermal mucin (both associated with CLE) may serve as helpful discriminators of CLE and IP. Previously described differences such as perieccrine lymphocytic infiltrate and vacuolar interface change (basal vacuolation and necrotic keratinocytes) are not reproducible in this series. Similarly, CD123 and CD30 immunostains fail to distinguish between CLE and IP.

540 Immunodetection of Mitotic Figures and G2+ Tumor Nuclei with Histone Markers in Stage III Melanoma Samples

Daniel Wimmer, Michael T Tetzlaff, Carlos A Torres-Cabala, Denai R Milton, Priyadharsini Nagarajan, Phyu P Aung, Victor G Prieto, Jonathan L Curry. The University of Texas MD Anderson Cancer Center, Houston, TX.

Background: Mitotic figure count is an important prognostic parameter in primary melanomas. Essential to mitosis and cell division is chromatin condensation regulated by posttranslational modification of histone tails. Surrogates of chromatin regulation by histone associated mitotic markers PHH3 (Ser10), H3K79me3T80ph (H3KT), and H3K9me3S10 (H3KS) appear in G2 through M phases of the cell cycle. The combined number of H3KT positive mitotic figures and G2+ tumor nuclei has been shown to be associated with more biologically aggressive primary melanomas. We sought to examine the significance of mitotic figure count and G2+ tumor nuclei in melanoma samples from stage III disease (regional lymph node metastasis) and correlated these values with known histologic parameters and clinical outcome.

Design: Tissue microarrays (TMA) composed of metastatic melanoma samples from 57 patients with stage III disease were subjected to immunohistochemistry with anti-PHH3, anti-H3KT, and anti-H3KS. Mitotic figure count and G2+ tumor nuclei were recorded per 3 mm diameter tissue core and comparisons were made using either Wilcoxon rank sum test or Kruskal Wallis test for categorical values and Pearson's correlations for continuous measures. Univariate Cox proportional hazard regression models were used to assess overall survival (OS) and progression free survival (PFS).

Results: Stage III melanomas were from 39 men and 18 women with median age of 55 years (range: 26 -84). The mean mitotic counts and G2+ tumor nuclei by anti-PHH3, anti-H3K79T, and anti-H3K9S are in table 1.

Table 1	PHH3 mean (SD)	H3KT mean (SD)	H3KS mean (SD)
Mitotic count	4.9 (5.6)	9.4 (8.1)	6.1 (5.8)
G2+ nuclei	0.7 (1.4)	80.8 (89.8)	1.5 (3.4)
Failed mitotic count	3.6 (3.1)	1.2 (1.5)	0.4 (0.8)

96% of patients had higher failure rate of detection of mitotic figures with PHH3 compared to H3KT and H3KS. Compared with PHH3 and H3KS, there was significant association with vertical growth phase of the primary tumor with combined H3KT mitotic figure count and G2+ tumor nuclei (p=0.019). No association with mitotic figure count or G2+ tumor nuclei was found with number or size of lymph node metastasis, OS or PFS.

Conclusions: Immunodection of mitotic figures was superior with H3KT and H3KS compared to PHH3; however, the mitotic figure count and/or G2+ tumor nuclei was not a strong predictor of a more biologically aggressive tumor or survival in stage III melanoma samples tested.

541 BRAF Mutation V600E Induces Expression Change of Signaling Transduction Molecules in Metastatic Melanoma Cell Lines

Chunhui Yi, Fei Ye, Qiong Gan, David Zhang. St. Luke's-Roosevelt Hospital, Mount Sinai Medical Center, New York City, NY; Mount Sinai Medical Center, New York City, NY.

Background: Approximately 40–50% of melanomas bear BRAF mutation. Among these, 70% -90% are V600E, which results in changes of several cascades of intracellular molecular singling pathways. It leads to the constitutively activation of its substrate Mek, and which in turn results in the activation of Erk and the suppression of Ras-GTP. These molecules have been therapeutic targets for metastatic melanoma, a devastating disease with a very poor prognosis. Identifying downstream alterations of the critical molecules in the signaling pathways in V600E mutation could result in the discovery of potentially novel therapeutic targets.

Design: To determine the signaling changes in BRAF mutation, we used four melanoma cell lines: primary melanoma cell line with wild-type BRAF (WM3862); metastatic melanoma cell lines with wild-type BRAF (MeWo); or V600E mutation (G361 and A2058). We designed an in-house protein array with the antibody of 137 most common

oncogenic, signaling proteins, and tumor suppressors. The expression of the 137 proteins were examined and compared in the four BRAF wild-type or V600E mutated melanoma cell lines.
Results: The result showed that there is a significant difference in protein expression in the BRAF wild-type cell lines versus the V600E mutated metastatic cell lines. Only 4 out of the 137 proteins are highly expressed in the wild-type BRAF cell lines (WM3862 and MeWo); whereas another 15 proteins are highly expressed in the BRAF V600E mutated metastatic cell lines (G361 and A2058). Taken together, BRAF wild-type and V600E melanoma could be characterized by these 19 proteins. Among the 15 genes highly expressed in V600E cells are p90RSK, an Erk inhibitor; p-GSK-3α/β, apoptosis regulator; Bax, another key regulator of apoptosis, cyclin-dependent kinase 1, a cyclin partner, NFκB, and other singling proteins.
Conclusions: BRAF mutation has been shown to be one of these key players of metastatic melanoma, contributing to the uncontrolled cell proliferation, resistance to apoptosis, and poor prognosis. Our knowledge of its effect on cell signaling is limited. Here we demonstrate that BRAF mutation V600E results in a significant changes in protein expression (19 out of 137 proteins, 13.87%) of apoptosis and signaling transduction in metastatic melanoma. The result may help illustrate how BRAF mutation affects singling and provide targets to inhibit its downstream partners.

Education

542 Correlation between USMLE Scores and Resident In-Service Examination (RISE) Scores: Should USMLE Scores Be Used as a Benchmark When Selecting Residents?

Yasemin Akdas, Kamran M Mirza, Guliz A Barkan. University of Florida, Gainesville, FL; Loyola University Medical Center, Maywood, IL.
Background: USMLE is an objective and numerical measure that allows unbiased comparison among candidates. Consequently, USMLE scores is an important criterion in selecting candidates for residency programs. It is often assumed that candidates with higher USMLE scores have superior academic skills and are more likely to perform better in RISE compared to their peers. The aim of this study was to assess if residents with higher USMLE scores performed better in RISE.
Design: All available USMLE and RISE scores of residents who have been training in our program from 2005 to 2015 were de-identified and tabulated. Residents who did not have USMLE scores (admitted via COMLEX scores only) were excluded from the study. To investigate the relationship between USMLE scores and RISE scores, we calculated each resident's mean RISE score for PGY1/PGY2, PGY3/PGY4, and PGY1-PGY4. Linear regression analyses in R-project were performed to investigate the association between USMLE and these three RISE metrics.
Results: There were a total of 40 residents training in our program during the time interval of the study. Four were excluded as they did not have USMLE scores available. 112 RISE scores were available for evaluation. There was a statistically significant association between USMLE scores and PGY1/PGY2 mean RISE scores (p-value=0.01), but this association was not observed for PGY3/PGY4 mean RISE scores (p-value=0.07). There was also no significant association between USMLE scores and PGY1-PGY4 mean RISE scores (p-value=0.08).
Conclusions: While USMLE may be the only uniform numerical measure that could be used to compare resident candidates across the board, our results show that there is only correlation between USMLE scores and RISE scores in the first two years of training. As the residents become PGY3 and PGY4, the residents with lower USMLE scores perform similarly to those with higher USMLE scores. This suggests that RISE scores do not depend on USMLE scores in the long run. Therefore, we recommend reducing reliance on these scores in the selection process. Similarly, USMLE scores of incoming residents may not be a good metric to evaluate the success of the graduate medical education programs.

543 Fine Needle Aspiration Cytology (FNAC) Simulation Using Phantoms. University Teaching Experience

Eduardo Alcaraz-Mateos, Alexandra Kundisova, Aleksijs Stopinskijs, Joanna Lenik, Iga Leszczynska, Iva Cerna, Martina Andrasova, Robert Roland, Agnes Gilberte, Cristina Martin, Mauricio Borbolla, Gerardo Valenzuela, Valeria Hernandez, Belen Roldan, Laura Martinez, Fuensanta Caballero. Morales Meseguer University Hospital, Murcia, Spain; University of Murcia, Murcia, Spain; Bratislava, Bratislava, Slovakia (Slovak Republic); Riga, Riga, Latvia; Krakow, Krakow, Poland; Prague, Prague, Czech Republic; Montpellier, Montpellier, France; Salamanca, Salamanca, Spain; Veracruz, Veracruz, Mexico; Juarez, Durango, Mexico; Zaragoza, Zaragoza, Spain; Castellón, Castellón, Spain.
Background: Fine needle aspiration cytology (FNAC) is a minimally invasive and extremely useful procedure with a low-risk of injury traditionally made by pathologists. The characteristics of pathology practices and limited equipment make teaching in this technique difficult, missing the opportunity to attract and recruit future pathologists. We therefore have introduced phantoms designed to perform FNAC in the educational process in our hospital.
Design: Phantoms are two life-sized hand-made anthropomorphic reproductions of a head & neck and a trunk, respectively, coated by silicone simulating skin with 8 inserted tumor areas (utility model ES1140059) in the cervical midline, retromandibular, supraclavicular, axillary (x2), breast, thigh and groin areas. They are inspired by other patents (US6485308,US5803746) and improved, including the whole FNAC process (palpation, puncture, aspiration, expel material on slide, and smear preparation), having human shape and being reusable. They allow performing FNAC, obtaining samples of cream material to be extended on slides. The practice was running in 2013/14 & 2014/15 academic years and consisted of obtaining an FNAC samples in a clinical context by each student individually, with a subsequent cytological correlation using whole slide imaging.
Results: 116 medical students, in their third year, from the University of Murcia, Spain, took part in the FNAC practice (16 groups: 66 women, 50 men). The success rate in the first attempt (puncture, aspiration of material, expelling and extending the obtained material on slides) was 96,5%. In Addition, 13 students from 10 other universities (national & international) conducted the same practice, referring to not having this opportunity in their places of origin and considering the practice to be valuable in an anonymous survey.
Conclusions: FNAC practices are easily implementable in the undergraduate curricula. There is no proper uniformity or standardization in the practices among different universities.
FNAC simulation provides students with greater knowledge and appreciation of our specialty.

544 Improving the Resident Selection Process

Candice C Black. Dartmouth Hitchcock Medical Center, Lebanon, NH.
Background: Residency Interviews require a substantial investment from a pathology department in the form of faculty time and departmental finances; in many cases including meals and / or hotels rooms. In an effort to decrease our overall investment, our residency program sought to increase the number of applicants per day and decrease the total number of interview days, keeping the remainder of the experience as stable from prior years as possible.
Design: We increased our number of applicants per day from 2.18 (average from past) weekday to approximately 10 per day on a Saturday morning. Other variables held constant included our paying for a hotel room for the night prior to interview, a dinner the night prior to interview, including "host" residents, 1 group introductory session, lunch the day of the interview, a tour of the facilities, two one-on-one faculty interviews, and a one-on-one closing with the program director or associate PD.
Results: We decreased our average number of interview days from 22 weekdays the year prior to 6 (3 Saturdays and 3 weekdays). We decreased our interviews from 48 (with 86 faculty interview hours, the year prior) to 33 (with 55.5 faculty interview hours). We ranked within the top 10 our NRMP list, an increase from our 40th position the year prior. Applicant feedback was very positive and included one comment stating that an applicant thought that the group interview made the position more desirable.
Conclusions: By changing our approach to the residency application process, we were able to decrease our departmental expenditures of time and money, and improve our overall result.

545 Pathology Knowledge Consumption Characteristics Online Using an Open Access Pathology Wiki

Michael Bonert, Vinita Parkash, Jens Schittenhelm. McMaster University, Hamilton, Canada; Yale University, New Haven, CT; University of Tuebingen, Tuebingen, Germany.
Background: An open access wiki-based website was launched one year ago to deliver anatomic pathology information to pathologists, pathology residents and medical students, and build a greater pathology knowledge commons that is accessible and easy to use.
Design: Detailed website usage information was collected including: what visitors viewed, how long they visited the site, how they connected to the site (search engine, external web site or bookmark), and the entry and exit pages. The top viewed pages were categorized and editor activity analyzed. Informally, pathologists were canvased, and responses on the site's twitter feed were examined.
Results: In the preceding year, the site had 205,000 visits, 2.0 million page views and 3.3 million hits from over 100 domains/countries. Monthly, the site averaged 9,000 unique visitors. The highest traffic pages related to benign gynecologic pathology and dermatopathology. High traffic was also seen on articles relating to ditzels, stains and histologic findings. Pages that present an overview of a topic were more often accessed from within the website. The percent visitors spending less than 2 minutes, between 2-15 minutes and more than 15 minutes was 84%, 8% and 8% respectively. Monthly, there were 2.0 visits per (unique) visitor, and 9.4 page views/visit. The top 10 percent of unique visitors were responsible for over half the page views. Approximately 30% of visitors came from a search engine. The content of the tweet with the most response dealt with image annotations. Relatively little interest was seen in response to an offline version of the site; however, site editors were enthusiastic. Approximately 18% of page views was by mobile devices or tablets.
Conclusions: The usage patterns suggest that site visitors directed to the site by a search engine have focused questions and move on quickly. The overview pages are utilized by visitors spending more time on the site, and probably viewed by individuals actively learning pathology. The relatively high views of benign gynecologic pathology, dermatopathology and ditzels, suggests these may be "pathologist specific areas" that are not well addressed by other web resources. Image annotations are considered valuable by pathologist users. A significant portion of people seeking pathology information are using mobile devices or tablets.